CONFIDENTIAL

RM A57J16

NACA RM A57J16

NACA

RESEARCH MEMORANDUM

TRANSONIC LATERAL AND LONGITUDINAL AERODYNAMIC CHARACTERISTICS OF A LATERAL-CONTROL SYSTEM EMPLOYING ROTATABLE AIRFOILS MOUNTED VERTICALLY AT THE WING TIPS OF AN UNSWEPT WING-FUSELAGE-TAIL COMBINATION

By John A. Axelson

Ames Aeronautical Laboratory
Moffett Field, Calif.

[redacted]

[redacted]

NATIONAL ADVISORY COMMITTEE
FOR AERONAUTICS

WASHINGTON

January 7, 1958

CONFIDENTIAL

NATIONAL ADVISORY COMMITTEE FOR AERONAUTICS

RESEARCH MEMORANDUM

TRANSONIC LATERAL AND LONGITUDINAL AERODYNAMIC CHARACTERISTICS OF A LATERAL-CONTROL SYSTEM EMPLOYING ROTATABLE AIRFOILS MOUNTED VERTICALLY AT THE WING TIPS OF AN UNSWEPT WING-FUSELAGE-TAIL COMBINATION

By John A. Axelson

SUMMARY

The aerodynamic characteristics of a new type of lateral control have been investigated throughout a Mach number range from 0.40 to 1.20. The control consisted of airfoils mounted vertically at the tips of the wing and could be rotated to induce rolling moments or lift on the wing surface. Two types of control airfoils were studied: one set having a chord equal to the wing-tip chord, the other set consisting of three smaller tandem-mounted airfoils whose combined chord equaled the wing-tip chord. The airfoils were investigated on the upper surface, the lower surface, and on both surfaces for a wide range of control deflections and angles of attack. The model had a Sears-Haack body of fineness ratio 12.4, an unswept wing of aspect ratio 3.10, taper ratio 0.39, and thickness-to-chord ratio 0.03, and had a cruciform tail. The control airfoils had a height one third of the tip chord of the wing. The control system gave lateral control generally comparable to that of conventional ailerons. Control reversal which occurred at 0.90 Mach number at 8° angle of attack was eliminated in the case of the large controls by deflecting only the lower controls, and in the case of the uniformly deflected multiple controls by changing to progressively increasing deflections of the tandem-mounted control airfoils.

INTRODUCTION

The lateral-control system for high-speed aircraft has generally been limited to either trailing-edge mounted ailerons, spoilers, or a combination of both. The conventional aileron operating in the boundary layer and wake of the wing is subject to deteriorations and nonlinearities in effectiveness at transonic speeds, and its location probably increases its vulnerability to buffet and flutter. At transonic and supersonic

speeds, the rearward travel of the center of pressure on the aileron and the adverse wing elastic deformation may lead to aileron control reversal. Aileron hinge moments and control forces change so erratically or become so large at high speeds that power-boost systems are used almost universally on high-speed aircraft. The spoiler does not provide a linear control; its effectiveness is usually reduced or reversed at higher angles of attack and it constitutes a likely source for buffet, as pointed out in references 1 and 2.

Efforts have been directed at developing other types of lateral controls, such as the differentially operated horizontal tail reported in reference 3 and differentially operated speed brakes reported in reference 4. A primary disadvantage of these controls is the interaction of the lateral with the longitudinal and directional characteristics. The speed-brake control, like the spoiler, is nonlinear and produces high drag with the prospect of adverse air flow and buffet at the tail. Air-jet or reaction type controls have been considered for very high altitude missile applications, but do not offer any distinct advantages for more conventional aircraft operating at lower altitudes.

The present report describes a new type of aerodynamic lateral control which consists of rotatable airfoils mounted vertically at the tips of the wing. The location of the controls offers distinct advantages in that at supersonic speeds it would allow a much greater influence to be exerted on the wing loading by control deflection than is possible with trailing-edge controls having supersonic hinge lines. The behavior of the controls may be explained as follows. A control mounted on the lower surface of the wing casts a compression shock wave or increased pressure on the wing lower surface when the control is toed out (i.e., control leading edge deflected away from the fuselage). A toed-in control on the wing upper surface casts an expansion or a reduction in pressure across its influence zone on the wing upper surface. Either or both of these controls thus increase the lift on the adjacent wing panel. When the controls at both wing tips are deflected to increase lift, no rolling moments should result. The lifting case has been treated in a parallel theoretical study reported in reference 5 where linearized or first-order theory has been applied to idealized wing-fuselage-fin arrangements. When the controls are deflected to increase the lift on one wing panel and decrease it on the other, roll control results. Both the lift and roll-control characteristics for several different control arrangements are studied in the present report.

NOTATION

b wing span

C_D drag coefficient, $\frac{\text{drag}}{qS}$

C_L lift coefficient, $\frac{\text{lift}}{qS}$

C_l rolling-moment coefficient about the body longitudinal axis, $\frac{\text{rolling moment}}{qSb}$

C_m pitching-moment coefficient about the lateral axis through $\frac{\bar{c}}{4}$, $\frac{\text{pitching moment}}{qS\bar{c}}$

C_n yawing-moment coefficient about the body vertical axis through the intersection of the pitching-moment axis and body longitudinal axis, $\frac{\text{yawing moment}}{qSb}$

c local wing chord

$\bar{c}$ wing mean aerodynamic chord, $\frac{\int_0^{b/2} c^2 dy}{\int_0^{b/2} c\, dy}$

q free-stream dynamic pressure

M Mach number

S wing area

y lateral distance along wing span

α angle of attack, deg

δ control deflection angle, deg

ψ angle of yaw, deg

$\frac{dC_L}{d\alpha}$ lift-curve slope

$\frac{dC_L}{d\delta}$ control lift-effectiveness parameter

$\frac{dC_l}{d\delta}$ control roll-effectiveness parameter

$\frac{dC_D}{dC_l}$ drag due to rolling-moment parameter

$\frac{C_{n_\delta}}{C_{l_\delta}}$ yawing moment due to rolling-moment control parameter, $\frac{dC_n/d\delta}{dC_l/d\delta}$

APPARATUS AND TESTS

Wind Tunnel

The investigation was conducted in the Ames 14-foot transonic wind tunnel, which is a closed-circuit return-type tunnel having a flexible-wall nozzle and a perforated test section and operating at atmospheric total pressure. The model was mounted on the sting-support system shown in figure 1(a), and the forces and moments were measured by means of an electrical strain-gage balance housed within the model.

Tests

The wind-tunnel test program included Mach numbers of 0.40, 0.80, 0.90, 1.00, 1.10, and 1.20, and angles of attack from 0° to 12° in 4° increments. The Reynolds number variations per foot are shown in figure 2, where the wing mean aerodynamic chord and control chords have been noted. Two basic types of runs were made: First the controls were deflected as a lateral control for producing a rolling moment, and second, they were deflected symmetrically to vary the lift on the model. The complete model was also rotated 90° on the sting and tested through yaw angles from -2° to $+6^\circ$ at an angle of attack of 0° with and without the upper and lower large controls.

Description of Model

The wing-body-tail configuration used as the test vehicle for the controls was geometrically similar but one half the size of the model reported in reference 6. The fuselage was a Sears-Haack body of fineness ratio 12.40 cut off at 90 percent of closure length for sting mounting and fitted with a boom at the nose. The wing of aspect ratio 3.10 and taper ratio 0.39 had a thickness-to-chord ratio of 0.03, a rounded leading edge, a mean aerodynamic chord of 1.41 feet, a span of 4.10 feet, and an area of 5.42 square feet. The leading edge was swept back 19.0° and the trailing edge was swept forward 12.5°. The cruciform tail configuration (fig. 1(a)) consisted of vertical and horizontal tails having quarter-chord lines swept back 45°. The vertical tail had an aspect ratio of 5.00, a taper ratio of 0.20, a span of 2.04 feet, and an NACA 65-009 section perpendicular to the quarter-chord line. The horizontal tail had an aspect ratio of 4.39, a taper ratio of 0.21, a span of 2.56 feet, and an NACA 65-006 section in the streamwise direction. Additional dimensional information may be obtained from reference 6. All control arrangements were tested on the model with tails on. In addition,

the combined upper and lower large controls with 8° deflection and the combined upper and lower multiple controls with uniform 8° and progressive 4°, 8°, and 12° deflections were tested with the tails removed.

Description of Control Surfaces

The support bodies which were attached to the wing tips of the model as shown in figure 1(b) consisted of conical forebodies and afterbodies of 19° total apex angle and a central rectangular portion containing the control turntables. Two sets of control airfoils were studied: One set shown in figure 1(b) had a 9-inch chord equal to the tip chord of the wing; the other set consisting of three smaller tandem-mounted airfoils shown in figure 1(c) had individual 3-inch chords and a combined chord of 9 inches. The control airfoils were flat steel plates having sharpened leading and trailing edges forming a wedge angle of 5°34' on the large controls and 6°44' on the multiple controls. All control airfoils extended 3 inches from the tip bodies and had a midchord thickness of 0.15 inch. Deflection angles were the same magnitude for all controls during each run, with the exception of the multiple controls which were also tested with progressively increased deflections. For this control configuration, the forward airfoils were set at 4°, the center airfoils at 8°, and the rear airfoils at 12°.

Corrections and Accuracies

The drag coefficients presented in this report have been corrected to a condition of free-stream static pressure at the base of the model. No corrections for wall-interference effects are deemed necessary, since the blockage was less than 0.3 percent. The results have been corrected for tunnel air-stream inclination, the correction decreasing with increasing Mach number from a value of 0.8° at 0.4 Mach number to 0° at 1.2 Mach number.

The accuracy of the results based on balance sensitivity and repeatability of data is believed to be within the following limits:

C_L	±0.01
C_D	±0.001
C_m	±0.005
C_l	±0.001
C_n	±0.001
M	±0.005
α	±0.1°

The rolling- and yawing-moment coefficients are referred to model axes, while the remaining coefficients are referred to the wind axes.

RESULTS

Lateral-Control Characteristics

Incremental rolling-moment coefficients as functions of control deflection for two arrangements of combined upper and lower controls are shown in figure 3. The average slopes of the curves of figure 3 in each of the 4° increments of control deflection are cross-plotted against Mach number in figure 4. Figures 5 and 6 present the incremental rolling-moment coefficients and effectiveness parameters, respectively, for the lower large controls and for the upper large controls tested separately. Figure 7 presents the variations with Mach number of the incremental rolling-moment coefficients for the combined upper and lower multiple controls uniformly deflected and progressively deflected. Incremental rolling-moment coefficients for the model with and without tail surfaces appear in figure 7 for the multiple controls and in figure 8 for the large controls. The variations with Mach number of the drag parameter dC_D/dC_l are shown in figures 9 and 10, while those of the yaw-due-to-roll parameter $C_{n_\delta}/C_{l_\delta}$ appear in figure 11. The variations of yawing-moment coefficient with angle of yaw are shown in figure 12 for the model with and without large controls for an angle of attack of 0°.

Lift-Control Characteristics

The lift curves of the basic model and of the model with several different control configurations are shown in figure 13. For these results the controls were deflected to influence the lift on both wing panels in a like manner with no resultant rolling moment. The variations of pitching-moment coefficient with lift coefficient for both lift-control and roll-control configurations are shown in figure 14. The variations with Mach number of lift-curve slope and of static longitudinal stability near zero lift appear in figure 15 and of control lift-effectiveness parameter in figure 16. Because of its relationship to wave drag, the longitudinal distribution of cross-sectional area of the model is presented in figure 17. The variations with Mach number of the drag coefficients for the basic model, for the model with control support bodies, and for the model with support bodies and undeflected controls are shown in figure 18. The effects of control deflection on the variations of drag coefficient with Mach number are shown in figure 19 for the model with large controls and in figure 20 for the model with multiple controls. The maximum lift-drag ratios for several model configurations appear in figure 21.

DISCUSSION

Lateral-Control Characteristics

Rolling effectiveness.- The incremental rolling-moment coefficients at angles of attack of 0° and 4° shown in figures 3(a) and 3(b) indicate that the combined upper and lower large controls and the combined upper and lower uniformly deflected multiple controls provided an effective and almost linear lateral control, with the former having the greater effectiveness. Figures 3 and 4 indicate a general reduction in effectiveness with increasing angle of attack and a reversal in effectiveness at high subsonic Mach numbers and 8° angle of attack with these particular control configurations on the test vehicle. The control reversal was considered to be due to adverse interference of the upper toed-in airfoil on the flow over the upper surface of the wing. The large controls were then studied separately on the upper surface and on the lower surface, with the results shown in figures 5 and 6. The reversal in effectiveness occurred again at a Mach number of 0.9 and an angle of attack of 8° with the upper controls, but no such reversal in effectiveness occurred with the lower controls at any test condition. Of significance is the fact that the effectiveness of the combined upper and lower arrangement was roughly equal to the sum of the effectiveness of the lower and that of the upper except where upper control reversal occurred near 0.9 Mach number.

For the multiple controls, it was reasoned that the supercritical flow conditions on the upper surface of the wing at 0.9 Mach number and 8° angle of attack might be influenced favorably if progressive deflection of the controls were used instead of the uniform deflection. The incremental rolling-moment coefficients for the combined upper and lower multiple controls with uniform 8° deflection and with progressive 4°, 8°, and 12° deflection are compared in figure 7. The reversal in effectiveness was eliminated by the progressively increased deflections of the tandem-mounted multiple controls. Although no hinge moments were measured in the present study, it is believed that the aft movement of the center of pressure during transition from subsonic to supersonic flight would entail combined hinge moments for the multiple controls which would be smaller than those for the large controls because of the smaller chords.

Because stall was well in progress on the wing of the test vehicle at subsonic Mach numbers at 12° angle of attack, rather large and inconsistent rolling moments occurred for the model without controls, making determination of the incremental rolling moments due to the controls uncertain. For this reason, incremental rolling-moment coefficients at 12° angle of attack were omitted from figures 3, 5, 7, and 8. Additional comments on the rolling moments developing on models in subsonic wind tunnels at angles of attack near the stall appear in reference 7. No

such erratic rolling moments occurred at Mach numbers of 1.0 or above, because of the improved lift characteristics of the basic model which became essentially linear over the test range of angles of attack as shown in figure 13.

The rolling effectiveness of the controls shown in figure 4(a) compares favorably with that of the ailerons of a low-aspect-ratio unswept-wing model reported in reference 8; however, the ratio of total control area to wing area in the present study was almost three times the ratio of aileron area to wing area of reference 8. The total aileron effectiveness $dC_l/d\delta$ from reference 8 at zero angle of attack was approximately 0.0015 for Mach numbers between 0.80 and 1.06, based on measurements at aileron deflections of -20°, -10°, 0°, and $+20^\circ$ only. (Whether adverse effects might occur at high subsonic Mach numbers and high angles of attack with smaller positive aileron deflections cannot be concluded from the limited results of reference 8.) Possible advantages offered by the lateral control of the present investigation are lower hinge moments and the opportunity to use full-span landing flaps.

Effect of tail surfaces on rolling effectiveness.- The incremental rolling-moment coefficients for the combined upper and lower multiple controls are shown in figure 7 and those for the combined upper and lower large controls are shown in figure 8 for the model with and without tail surfaces. The results indicate that the tail surfaces generally had a very small adverse effect on the lateral control effectiveness. Because the lateral controls were mounted at the wing tips, the vortices and wakes emanating from them did not pass close to the tails.

Lateral-control drag.- Although lateral controls are generally deflected for relatively brief time durations, and their drag may not be important from an aerodynamics standpoint, controls having high drag and producing extensive turbulence might be expected to require heavier and more rigid structures. The relatively small drag increments accompanying control deflection for the present controls have been combined with the rolling-moment increments to give the derivative dC_D/dC_l shown in figure 9 for the large controls and in figure 10 for the multiple controls. The drag of spoiler-type controls is generally directly proportional to the rolling effectiveness with corresponding typical values for dC_D/dC_l of around 2. The results in figures 9 and 10 indicate that little or no drag penalty occurred for small deflections of the present controls and that the drag-roll parameter generally exceeded unity only at control deflections of 12°.

Yawing moment due to rolling moment.- The variations of yaw-roll parameter $C_{n_\delta}/C_{l_\delta}$ shown in figure 11 indicate that little or no yawing moment accompanied deflection of the controls for angles of attack near 0°. As the angle of attack was increased, the combined upper and lower controls behaved similarly to ailerons in that adverse yawing moments

resulted, because the wing panel having the greater lift also had the greater drag component. The aerodynamic forces on each control airfoil also influenced the resultant yawing moment. The more rearward location of the force on the upper control airfoil at supersonic speeds produced an adverse yawing moment which added to that of the wing loading as indicated in figure 11(d). At subsonic speeds the lower controls produced adverse yawing moments which became much smaller at supersonic speeds.

There are four aspects of the behavior of the controls which bear mentioning. First, as already mentioned, at increasing angles of attack, the drag component of the wing panel carrying the greater normal force produced adverse yawing moments. Second, the air forces on each of the control airfoils differed at angle of attack, because the flow around the tip of the wing associated with the wing-tip vortex altered the actual deflection angle at which the control airfoils operated. (This flow inclination reinforced or added to the deflection angles and to the forces on those controls deflected to increase lift on a wing panel, but opposed or decreased the effective deflection angles and the forces on those control airfoils deflected to decrease wing-panel lift.) Third, the low pressure side of the control airfoil would be expected to have produced a greater force at subsonic speeds than the high pressure surface, a behavior similar to the distribution of lift between the upper and lower surfaces of an airfoil operating at subsonic speeds. At increasing supersonic speeds, the high pressure surface would exert increasingly greater influence as is the case for an airfoil operating at these speeds. Fourth, there were no sidewash or interference effects of the controls on the tail surfaces except at higher angles of attack and supersonic speeds where a small favorable effect occurred.

Yawing moment due to yaw angle.- The combined upper and lower controls had essentially no effect on static directional stability at 0° angle of attack as indicated in figure 12. If higher angles of attack had been tested, there appears to be little likelihood that any significant effects on yawing moment would have resulted within the Mach number range of the present test. Important to recognize, however, is the fact that if only upper controls or lower controls were used, there would have resulted a dihedral effect and a rolling moment.

Lift-Control Characteristics

Lift curves.- The variations of lift coefficient with angle of attack shown in figure 13 demonstrate the degree to which the lift of the test model was varied by symmetrical deflection of the controls. There were two ways in which the controls changed the lift characteristics of the test model. First, the lift-curve slope was increased by the controls as shown in figure 15(a). The results show that the controls contributed an end-plate effect which increased the effective aspect ratio of the

wing-control combination. Slightly larger end-plate effect resulted when the controls were deflected to increase the lift, except in the case of the multiple controls uniformly deflected 12° (upper controls toed in 12°, lower controls toed out 12°) where a reduction in lift-curve slope from the controls-neutral condition occurred. Additional information on the low-speed effects of symmetrically deflected end plates may be found in reference 9.

The second way in which the controls varied the lift on the model is shown in figure 16, where the rate of change of lift coefficient due to control deflection is presented for the combined upper and lower controls. The adverse effects of the upper toed-in controls at 8° angle of attack and 0.9 Mach number are evident, and are perhaps more severe than in the roll case where the upper control was toed-in at but one wing tip at a time. As was shown in the discussion of rolling effectiveness, the adverse effects on lift at high angles of attack and high subsonic Mach numbers could probably be reduced by deflecting only the lower controls at these conditions. The total lift increments produced by the addition of the controls to the test model then were the sum of the end-plate effects shown in figure 15(a) and the additional effects of control deflection shown in figure 16.

Static longitudinal stability.- The variations of pitching-moment coefficient with lift coefficient in figure 14 and the cross plots of the stability parameter dC_m/dC_L in figure 15(b) indicate that adding the controls increased the static longitudinal stability of the model for lift coefficients up to about 0.4 for all test Mach numbers. The results for the basic model are shown for Mach numbers of 0.6 and above. Results for several representative arrangements of combined upper and lower controls are presented in figure 14 for both symmetrical deflection of the controls to produce lift and for differential deflection of the controls to produce roll. At the larger lift-control deflections, the controls produced a negative trim change at the higher Mach numbers. Similar negative pitching moments occur with deflected conventional trailing-edge flaps having supersonic hinge lines. No adverse pitching moments occurred, however, when the present controls were deflected for roll control, as indicated by the flagged symbols of figure 14.

Drag.- Since the primary purpose of the present investigation was to assess the lateral control characteristics of the controls, no extra effort was directed at obtaining configurations having minimum drag. It may be seen in figure 17 that the additional frontal area of the controls aggravated the already unfavorable longitudinal area distribution of the wing-body combination used as the test vehicle. The variations of drag coefficient with Mach number in figure 18 show that a drag penalty occurred due to the addition of the control support bodies. The addition of the combined upper and lower large controls at 0° to the support bodies reduced the drag penalty at subsonic speeds. At the higher lift coefficients, the drag of the model with controls was generally less than that

of the basic model in spite of the less favorable longitudinal area distribution. As shown in figures 19 and 20, the drags for several different control configurations were less than that of the basic model at lift coefficients of 0.6 and 0.8, except for the range of Mach numbers from 0.80 to 0.95. The lower drags at the high lift coefficients were probably due in part to the increased lift-curve slopes and the lower angles of attack required to obtain a given lift coefficient with the control-equipped model. Lower angles of attack and lower drags at high lift coefficient offer possibilities for increasing the ceiling of an aircraft.

Maximum lift-drag ratio.- Since no fuselage contouring in accordance with the area rule was made to minimize the drag of the control-equipped model, and because the maximum lift-drag ratios occurred at low lift coefficients as shown in figure 21(b), there was a general reduction in maximum lift-drag ratio accompanying the addition of the controls (fig. 21(a)). A significant increase in the lift coefficient for maximum lift-drag ratio occurred, however, when the controls were added, as evident in figure 21(b).

CONCLUDING REMARKS

A study of the aerodynamic characteristics of a new type of lateral control employing vertically mounted, rotatable airfoils at the tips of the wing indicates that effective and essentially linear control was achieved with various control arrangements over most of the test Mach number range from 0.40 to 1.20. Control reversal which occurred at 0.90 Mach number at 8° angle of attack was eliminated in the case of the large controls by deflecting only the lower controls, and in the case of the uniformly deflected multiple controls by changing to progressively increasing deflections of the tandem-mounted control airfoils. The controls provided lift control as well as lateral control, and produced no serious effects on static longitudinal or directional stability. The controls and supporting wing-tip bodies caused a drag penalty at low lift coefficients which reduced the maximum lift-drag ratio. There was little or no additional drag penalty when the controls were deflected for roll control. At high lift coefficients, when deflected to control lift, the controls reduced the drag.

Ames Aeronautical Laboratory
National Advisory Committee for Aeronautics
Moffett Field, Calif., Oct. 16, 1957

REFERENCES

1. James, K. W.: Some Recent Information on Spoiler Controls With Particular Reference to Supersonic Speeds. R.A.E. TN Aero 2455, July 1956.

2. Rockwell, Robert W.: Analysis of Controllable Approach Drag Devices and High Speed Lateral Control Spoilers. Boeing Document WD-13368, Feb. 1956.

3. Campbell, John P.: The Use of the Horizontal Tail for Roll Control. NACA RM L55L16a, 1956.

4. West, F. E., Jr., and Critzos, Chris C.: Force Test Results for Body-Mounted Lateral Controls and Speed Brakes on a 45° Swept-Wing Model at Mach Numbers From 0.80 to 0.98. NACA RM L56I05, 1956.

5. Rossow, Vernon J.: A Theoretical Study of the Lifting Efficiency at Supersonic Speeds of Wings Utilizing Indirect Lift Induced by Vertical Surfaces. NACA RM A55L08, 1956.

6. White, Maurice D.: A Flight Investigation at Transonic Speeds of the Aerodynamic Characteristics of a Model Having a Thin Unswept Wing of Aspect Ratio 3.1. NACA RM A54E12, 1954.

7. Sears, W. R.: Some Recent Developments in Airfoil Theory. Jour. Aero. Sci., vol. 23, no. 5, May 1956, pp. 490-499.

8. Arabian, Donald D., and Schmeer, James W.: Lateral Stability and Control Measurements of a Fighter-Type Airplane With a Low-Aspect-Ratio Unswept Wing and a Tee-Tail. NACA RM L55F08, 1956.

9. Clements, Harry R.: Canted Adjustable End Plates for the Control of Drag. Aero. Engr. Rev., vol. 14, no. 7, July 1955, pp. 40-44.

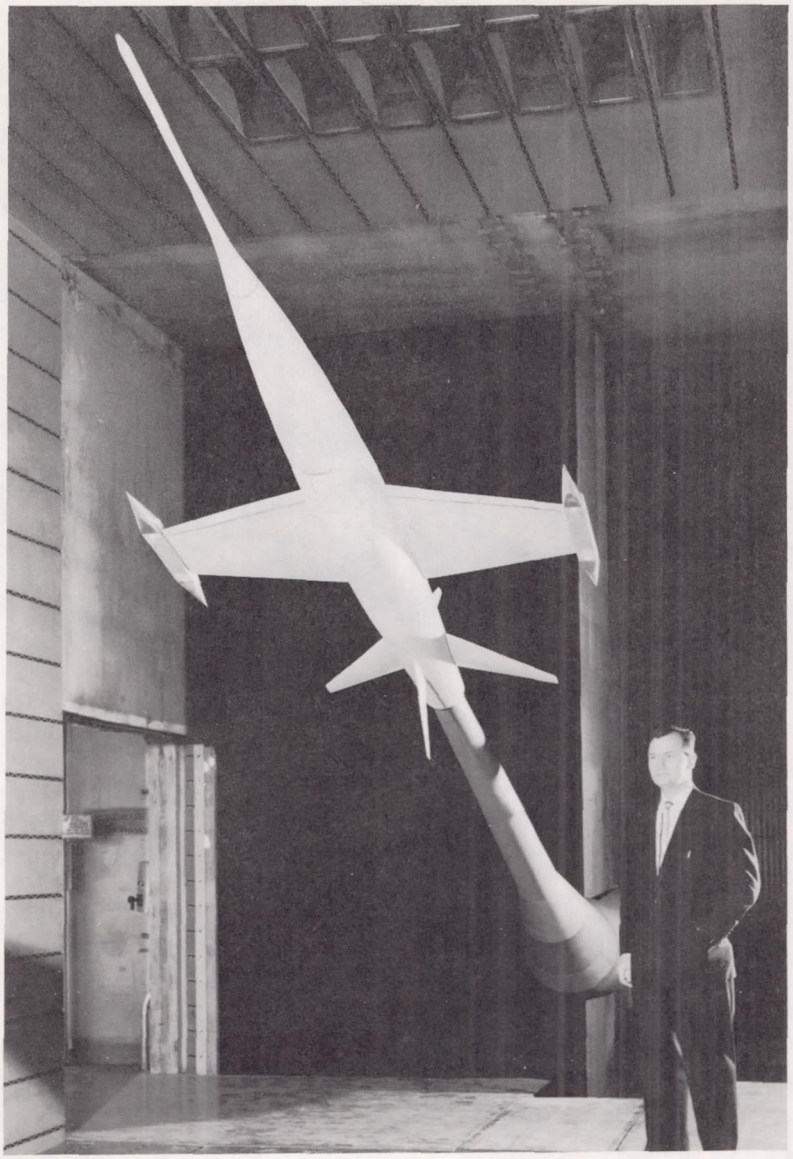

A-20978

(a) Model with control support bodies attached to the wing tips.

Figure 1.- Photographs of the model and the test-section installation.

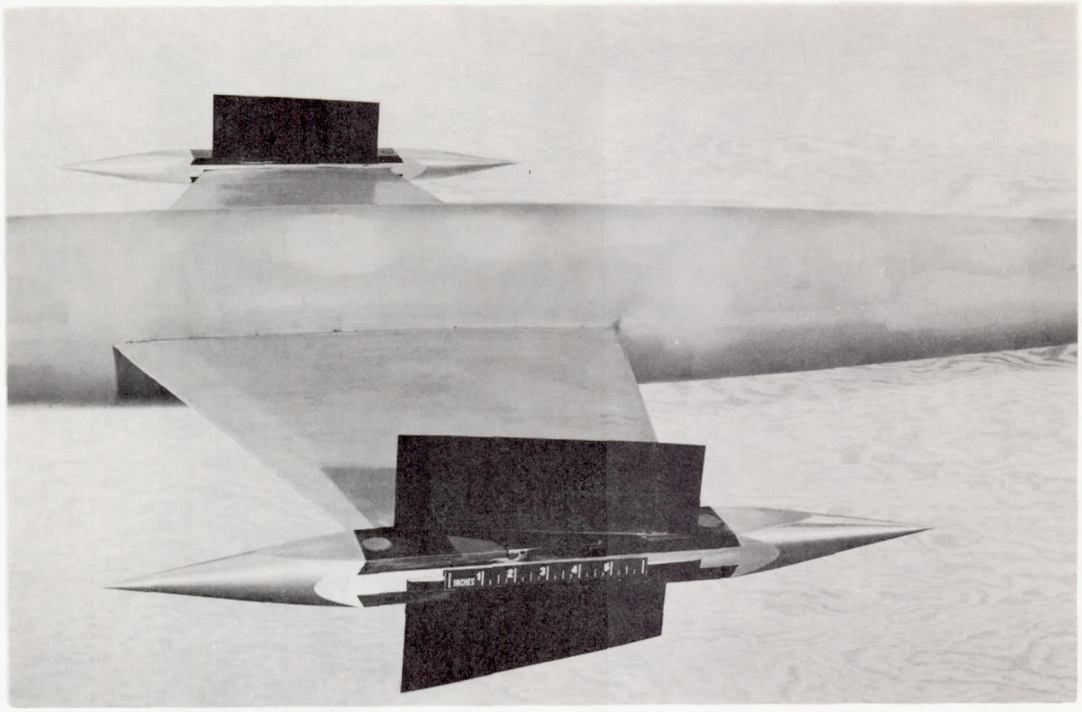

(b) Close-up view of large controls. A-21131

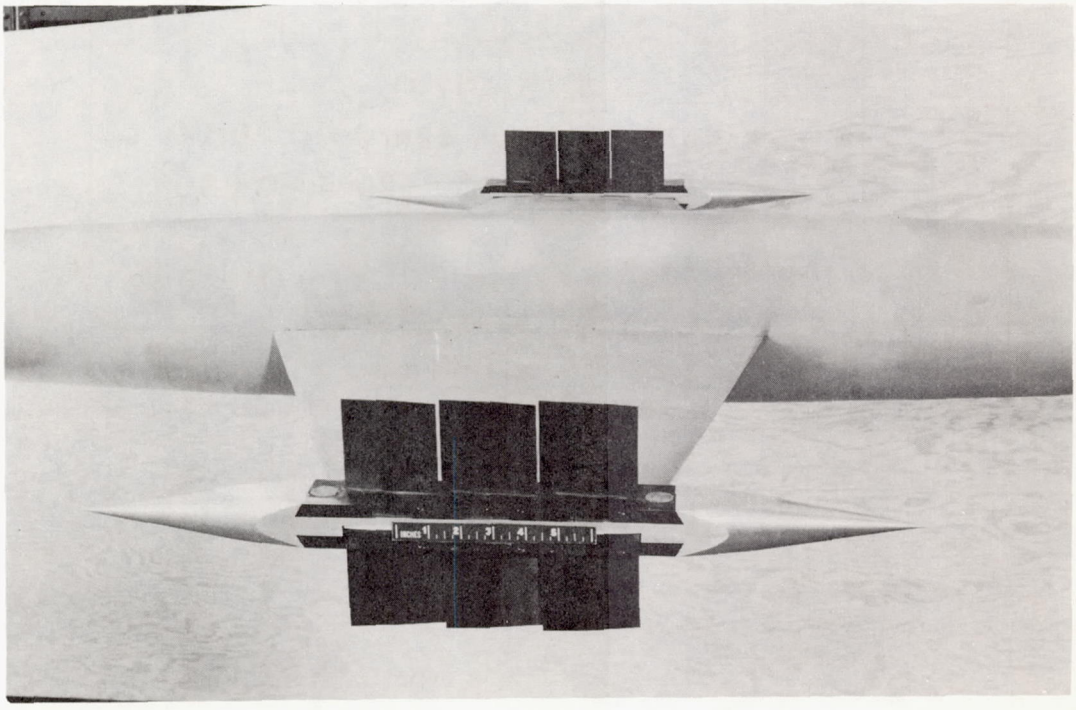

(c) Close-up view of multiple controls. A-21132

Figure 1.- Concluded.

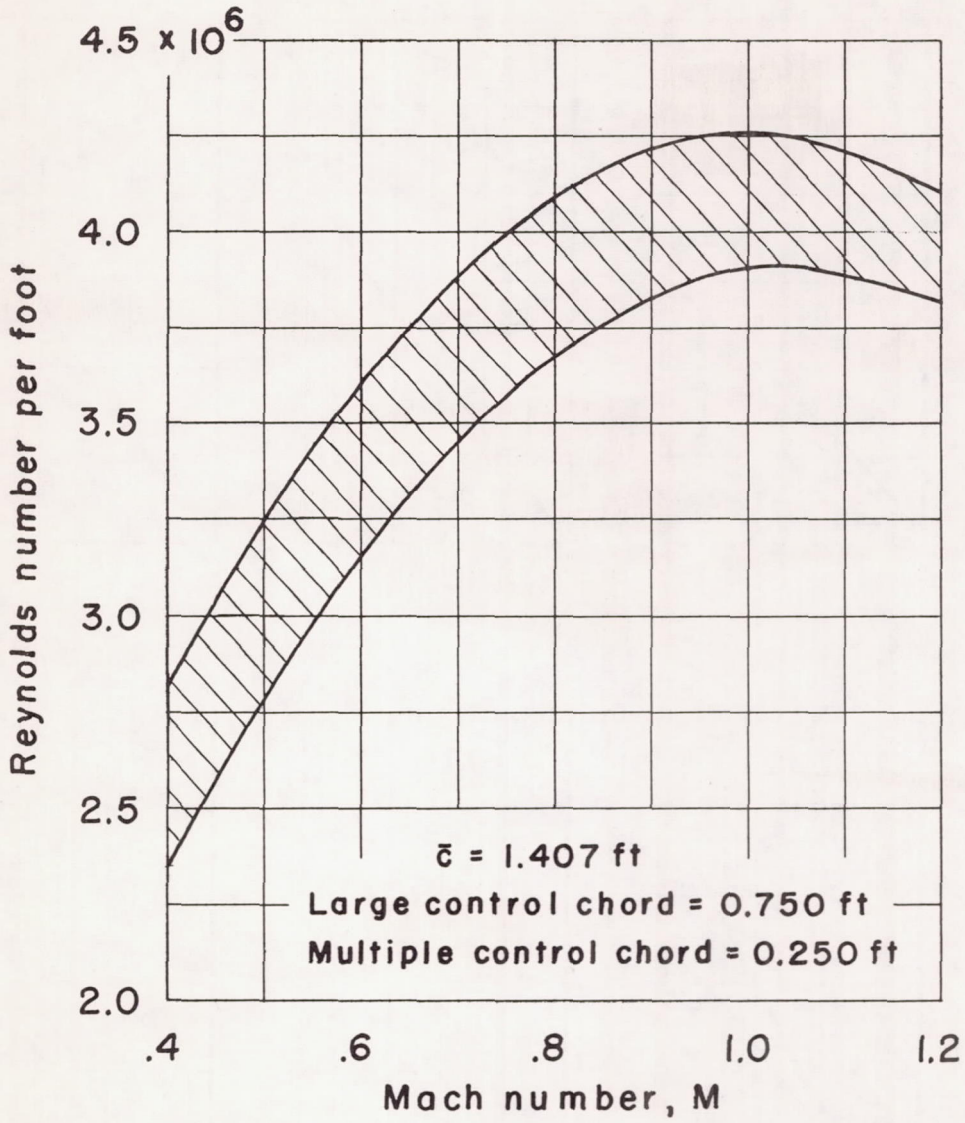

Figure 2.- Variations of Reynolds number with Mach number.

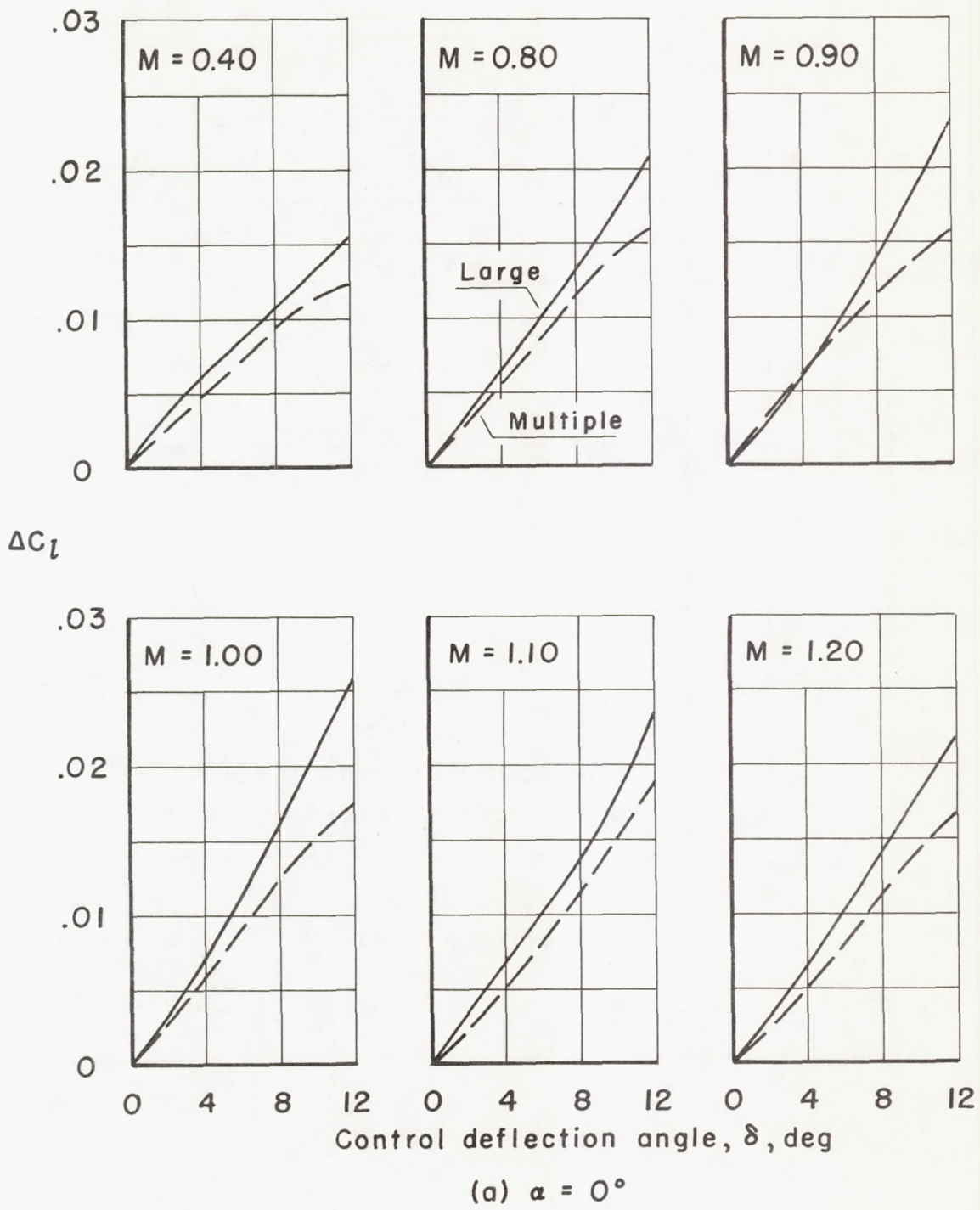

Figure 3.- Variation of incremental rolling-moment coefficient with control deflection for combined upper and lower large controls and for uniformly deflected multiple controls.

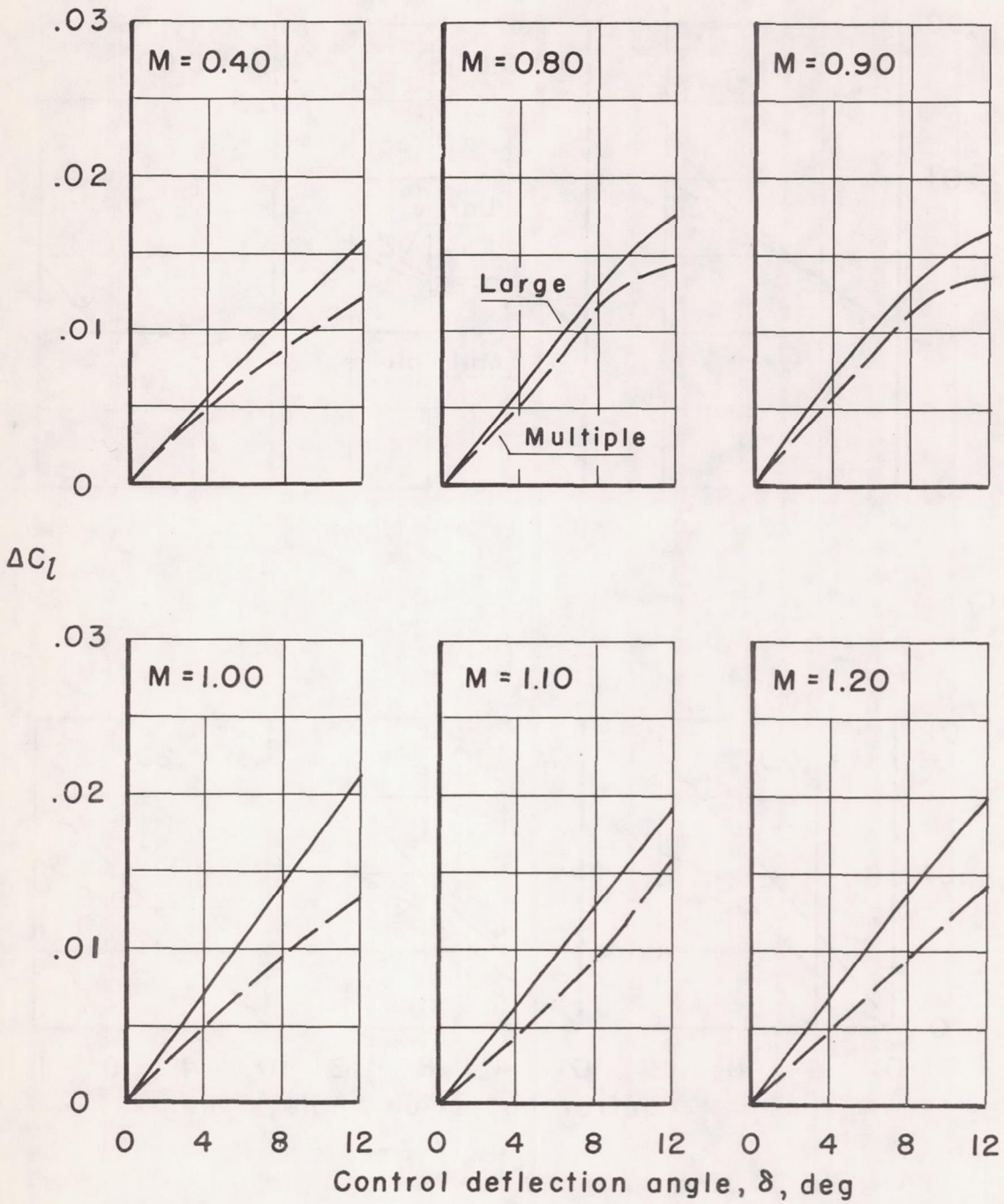

(b) $\alpha = 4°$

Figure 3.- Continued.

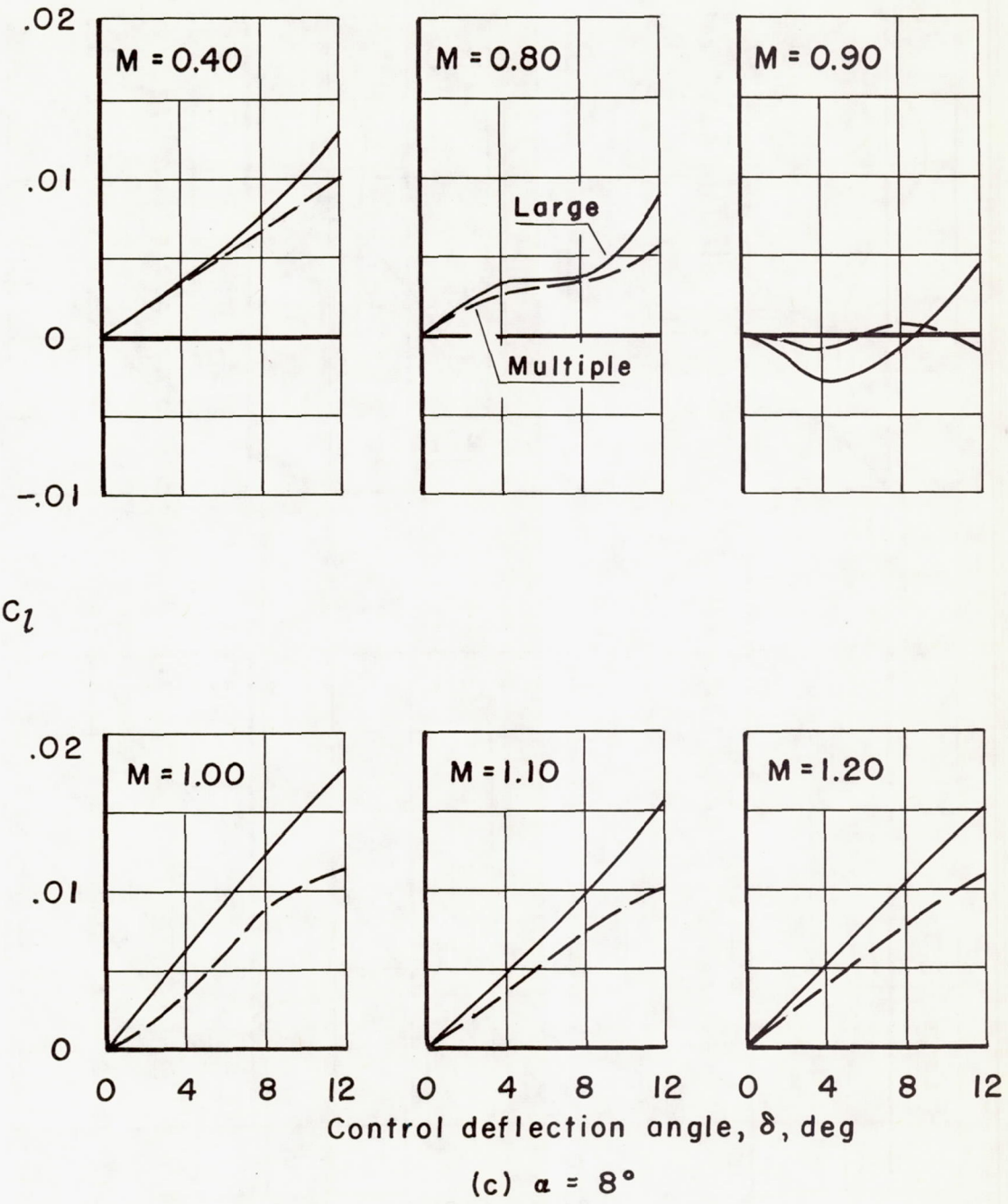

(c) $\alpha = 8°$

Figure 3.- Concluded.

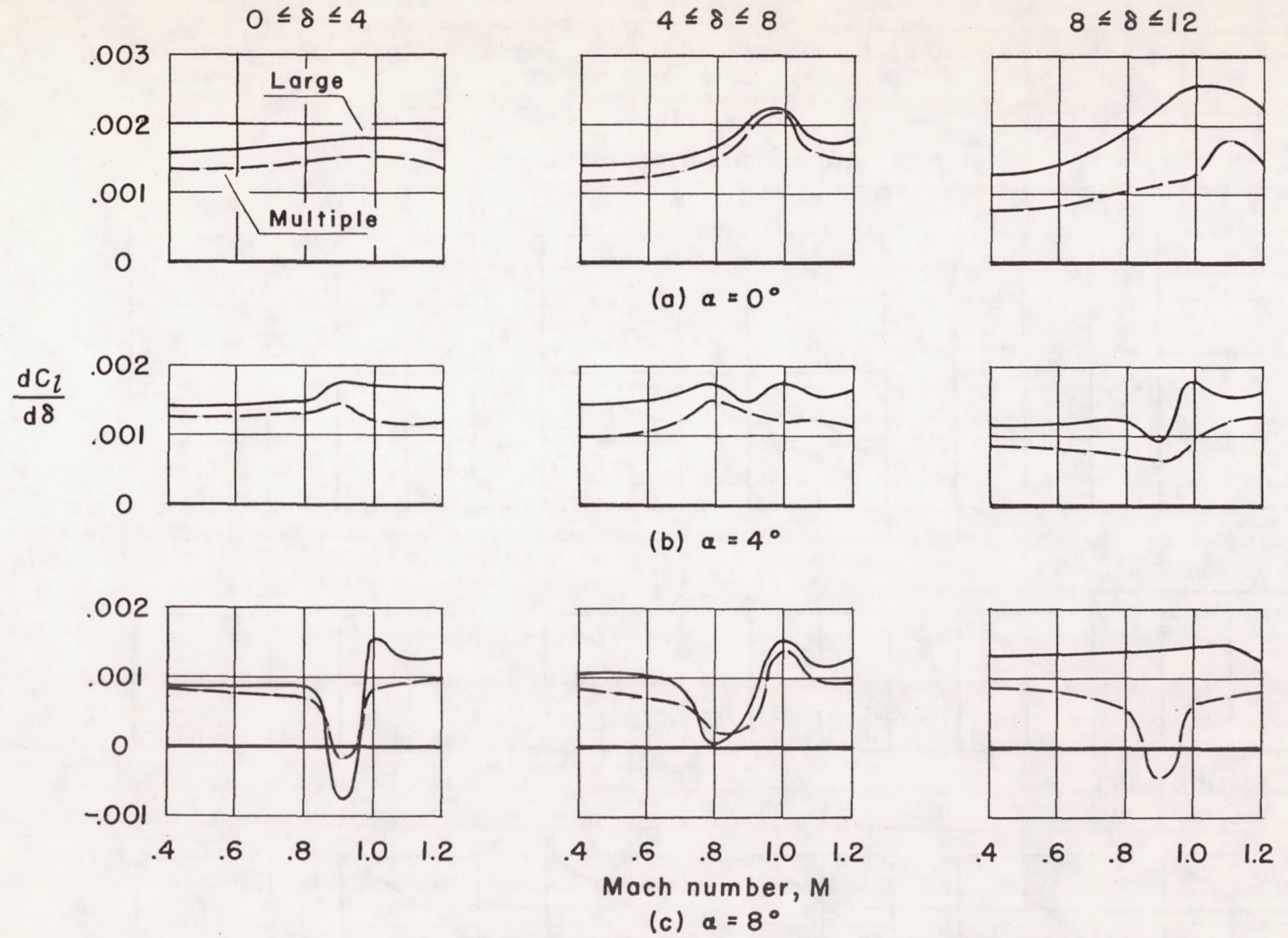

Figure 4.- Variation of lateral-control effectiveness with Mach number for combined upper and lower large controls and uniformly deflected multiple controls.

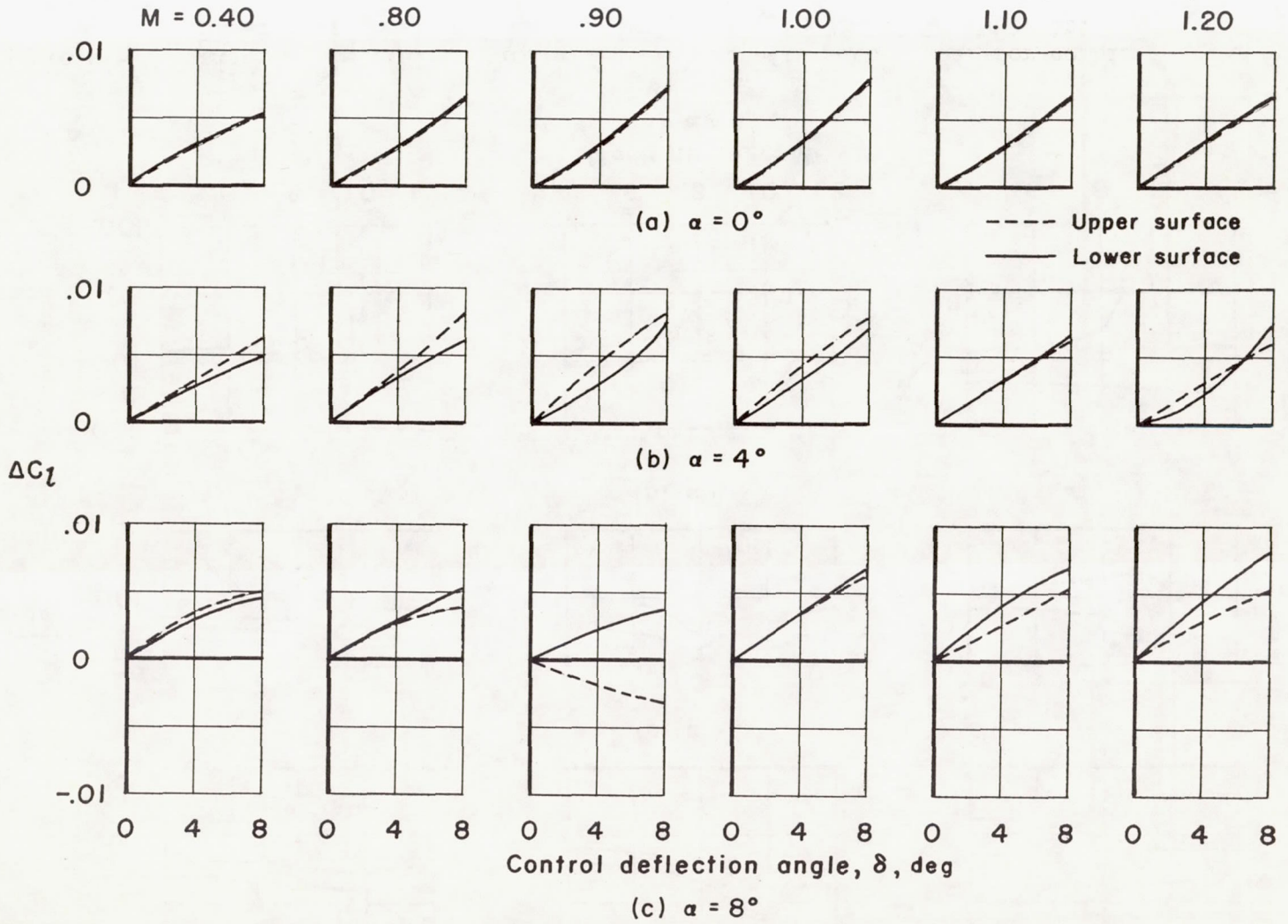

Figure 5.- Comparison of the incremental rolling-moment coefficients for the large controls on the upper and on the lower wing surface.

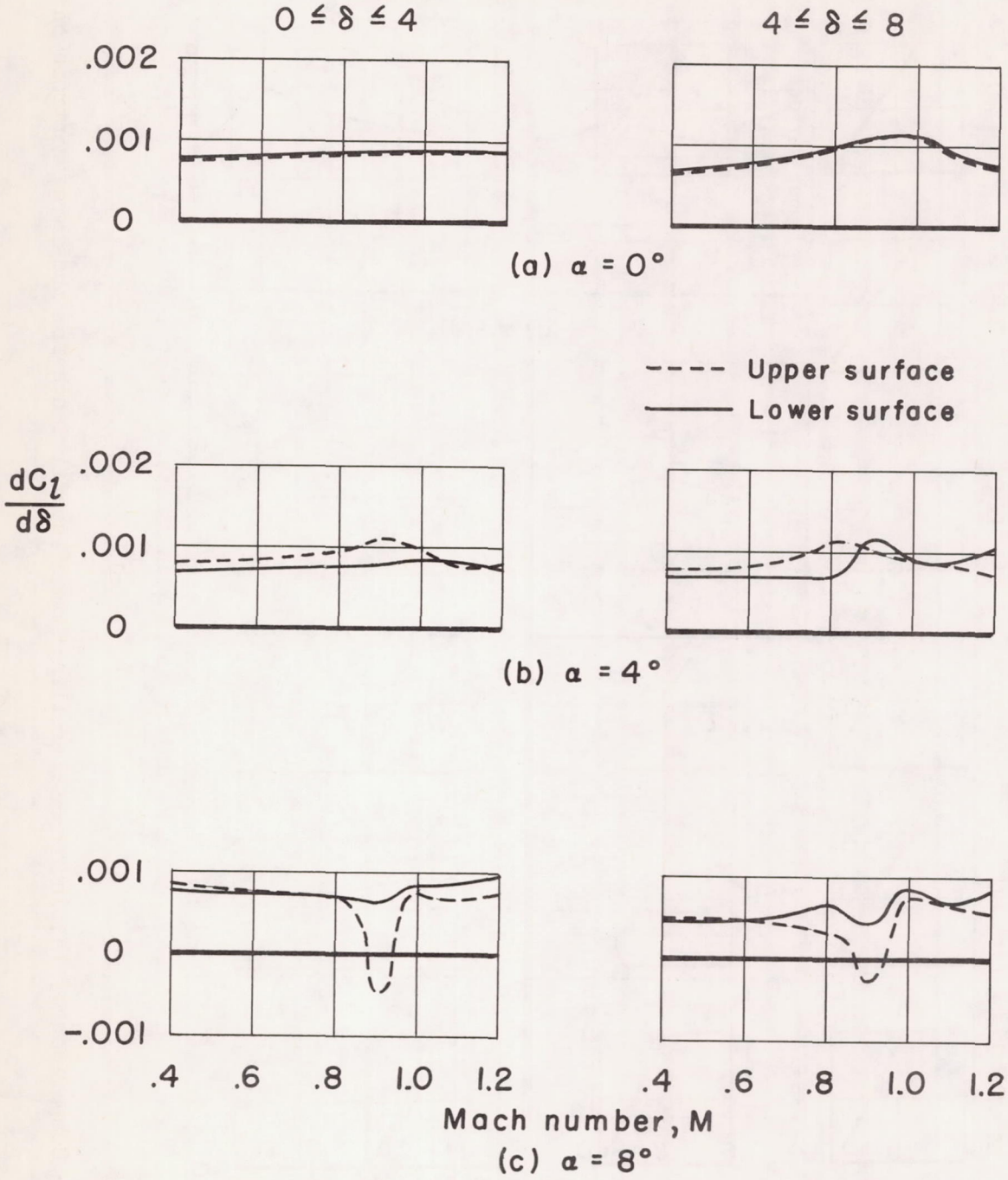

Figure 6.- Variation of lateral-control effectiveness with Mach number for large controls on one wing surface only.

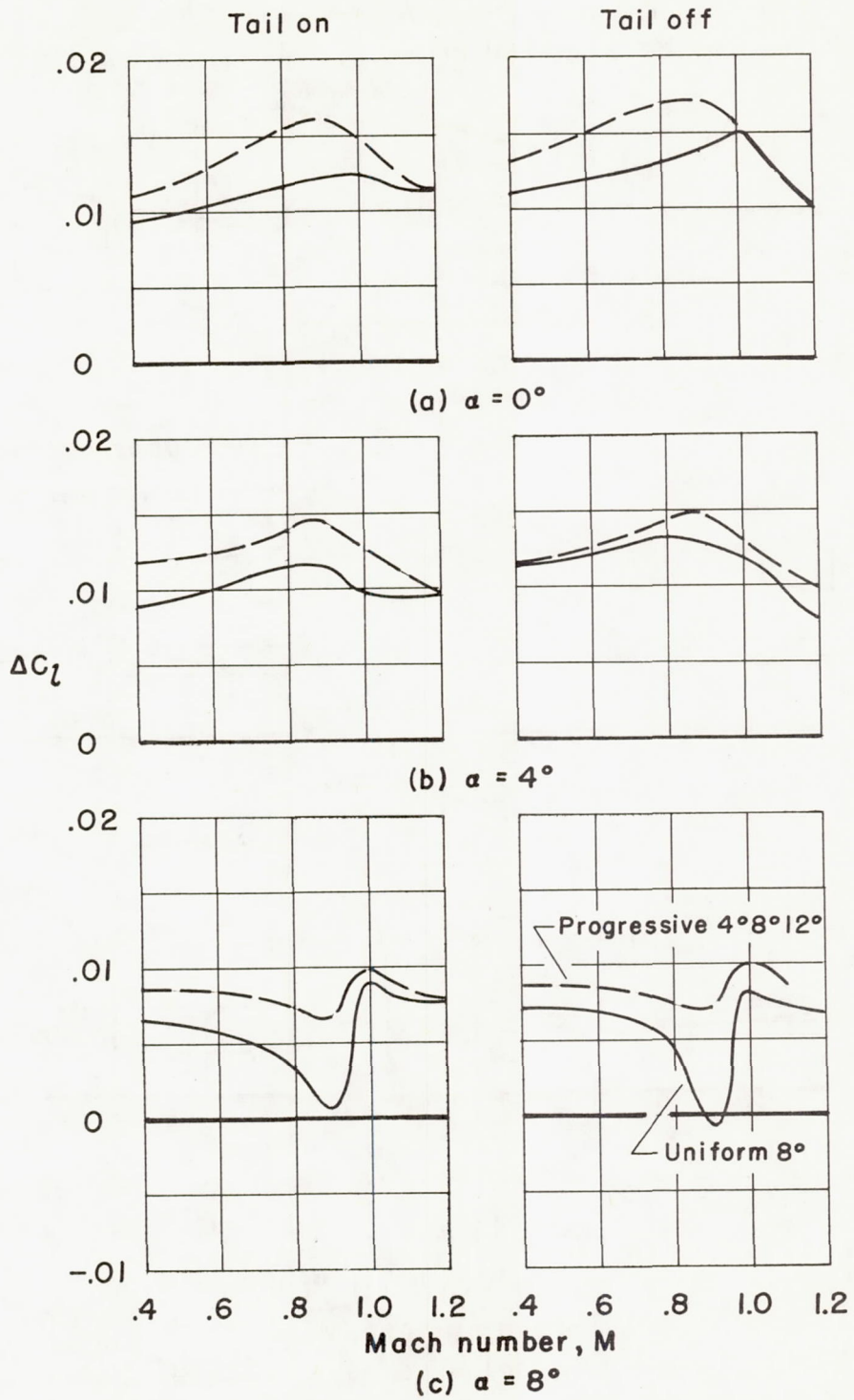

Figure 7.- Variation of incremental rolling-moment coefficient with Mach number for combined upper and lower multiple controls having a uniform 8° deflection and a progressive 4°, 8°, and 12° deflection.

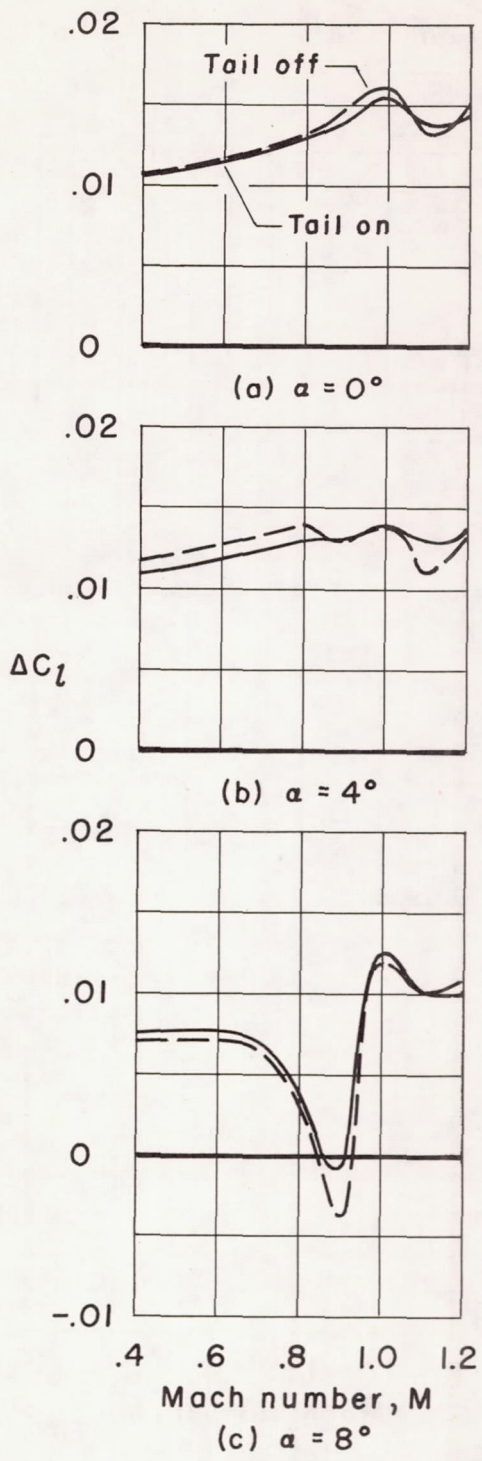

Figure 8.- Effect of tail surfaces on the variation of incremental rolling-moment coefficient with Mach number for combined upper and lower large controls deflected 8°.

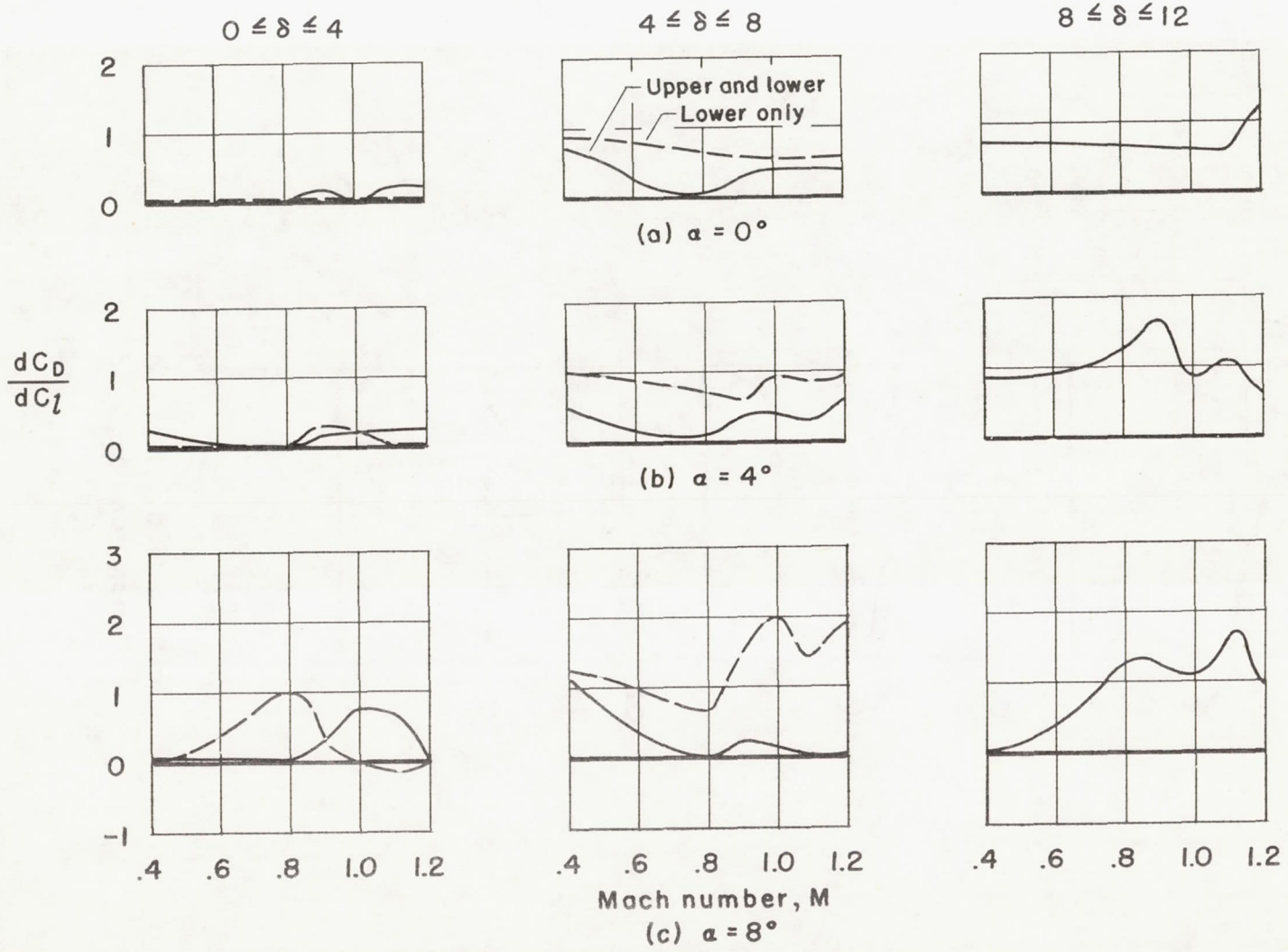

Figure 9.- Variation of drag-roll parameter with Mach number for large controls on the lower wing surface and on both wing surfaces.

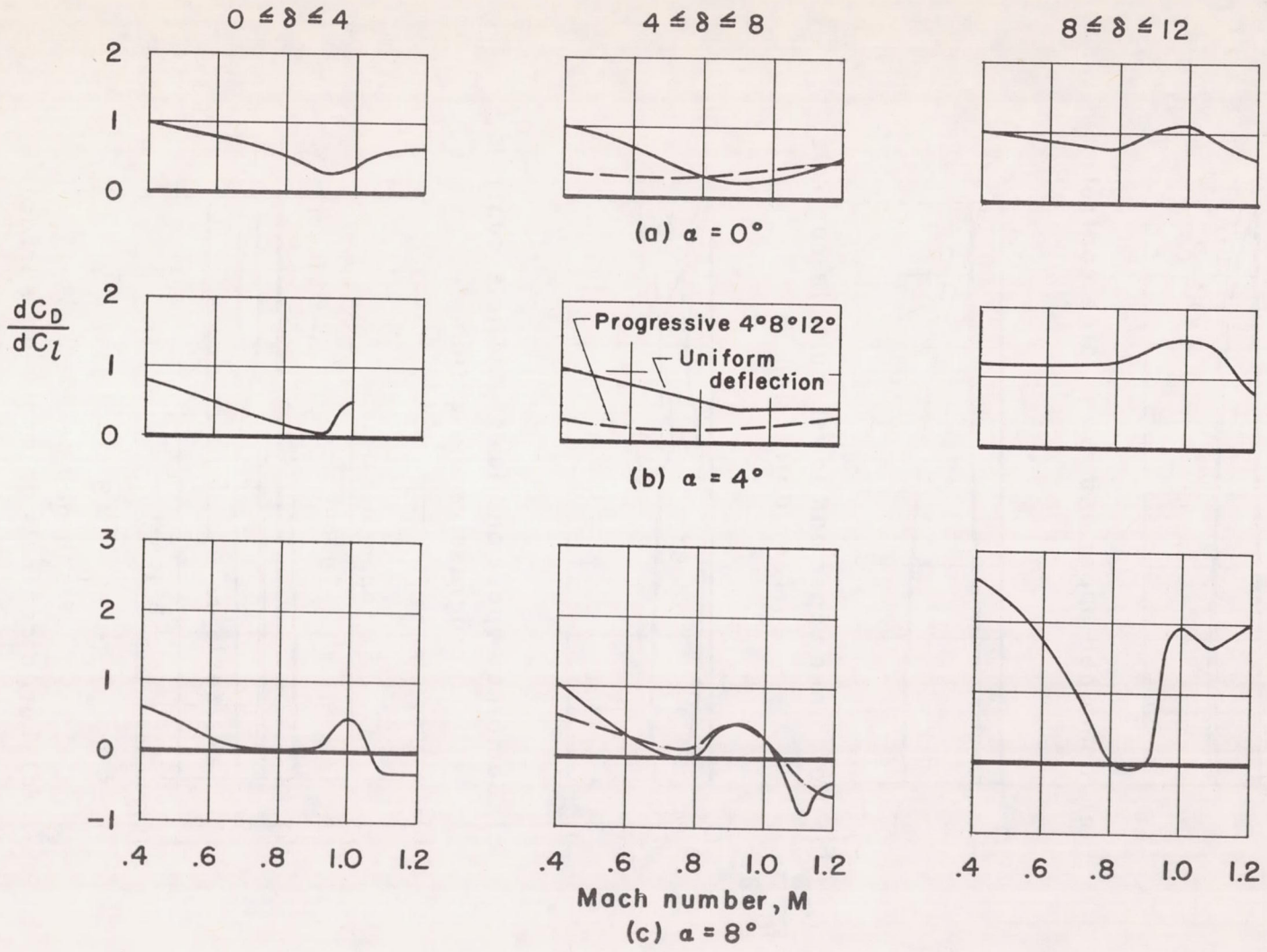

Figure 10.- Variation of drag-roll parameter with Mach number for combined upper and lower multiple controls.

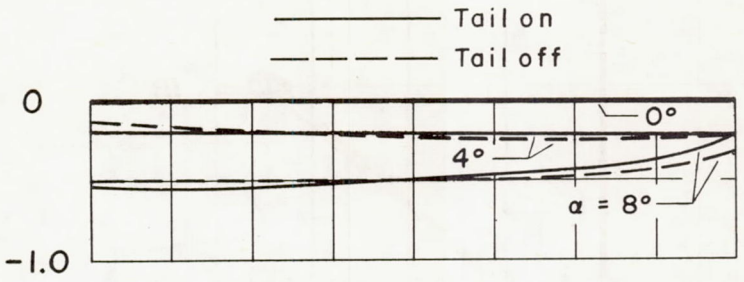

(a) Combined upper and lower large controls.

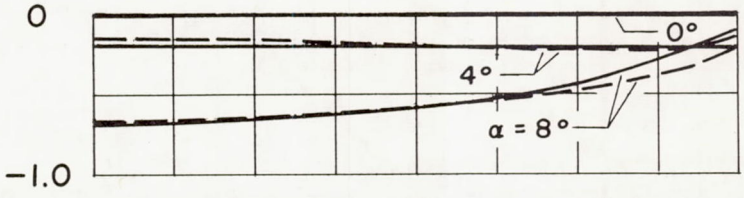

(b) Combined upper and lower multiple controls, uniform deflection.

$\frac{C_{n_\delta}}{C_{l_\delta}}$

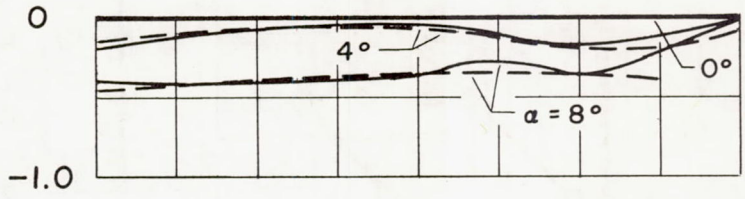

(c) Combined upper and lower multiple controls, progressive deflection.

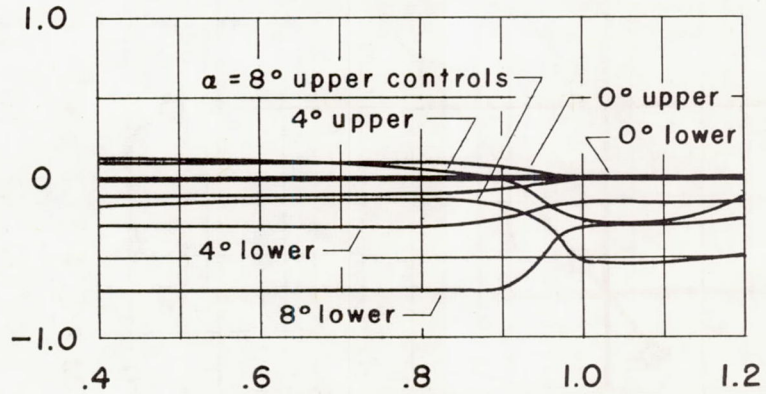

(d) Large controls on one wing surface.

Figure 11.- Variation with Mach number of yawing moment due to rolling moment.

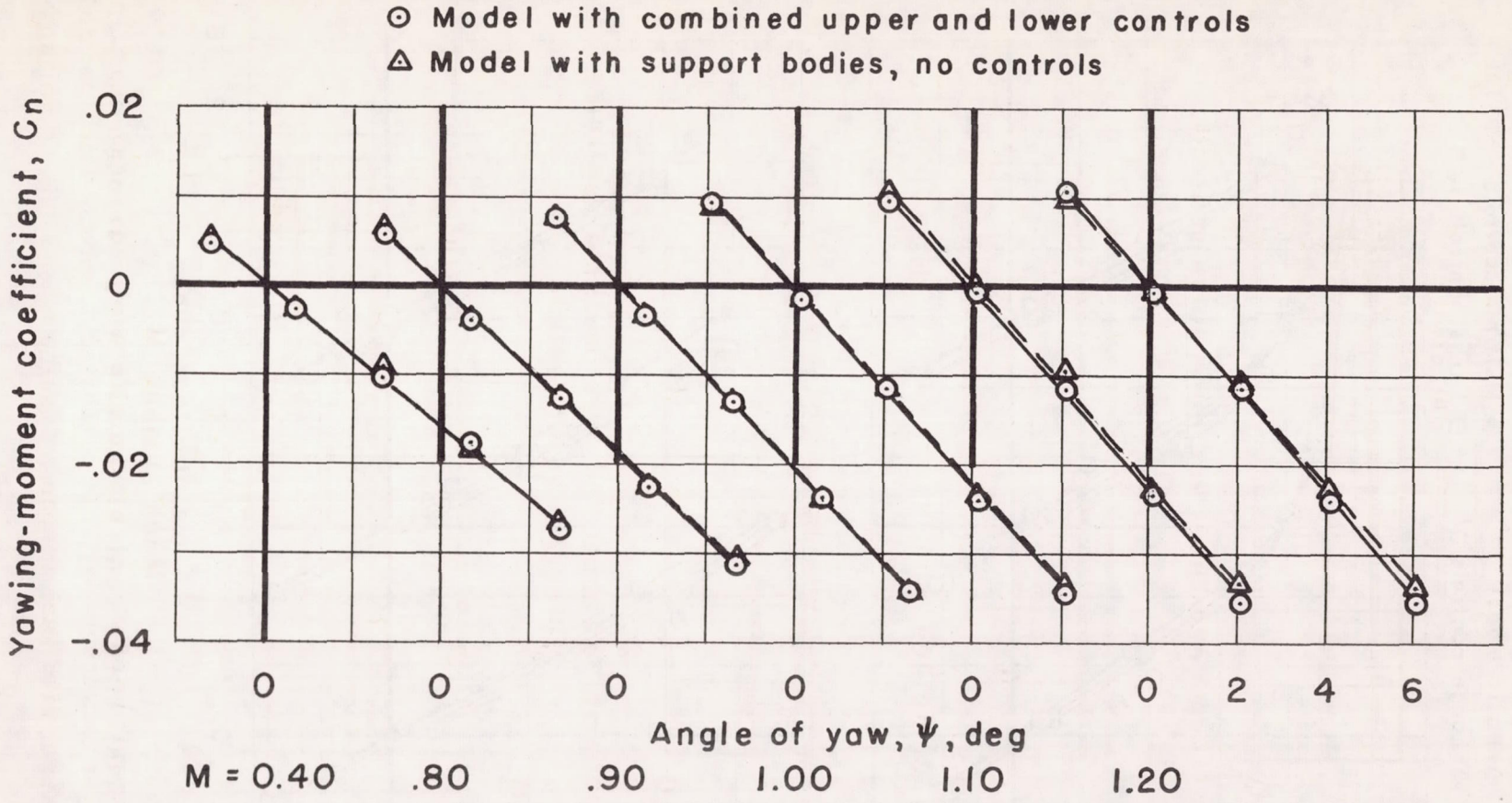

Figure 12.- Variation of yawing-moment coefficient with yaw angle for the model with and without combined upper and lower large controls; $\alpha = 0^\circ$, $\delta = 0^\circ$.

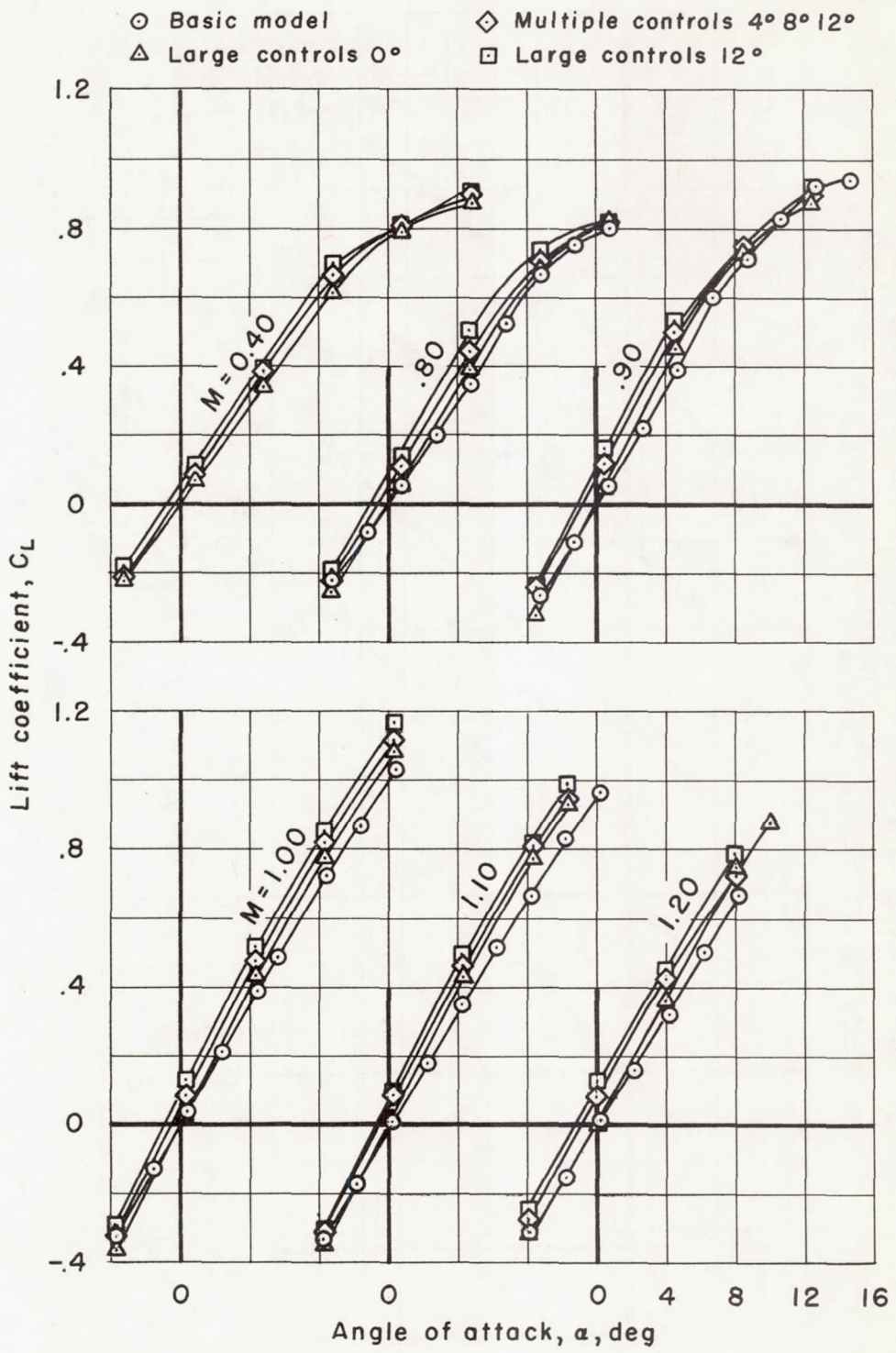

Figure 13.- Comparison of the lift curves for the model with and without combined upper and lower controls deflected to produce incremental lift.

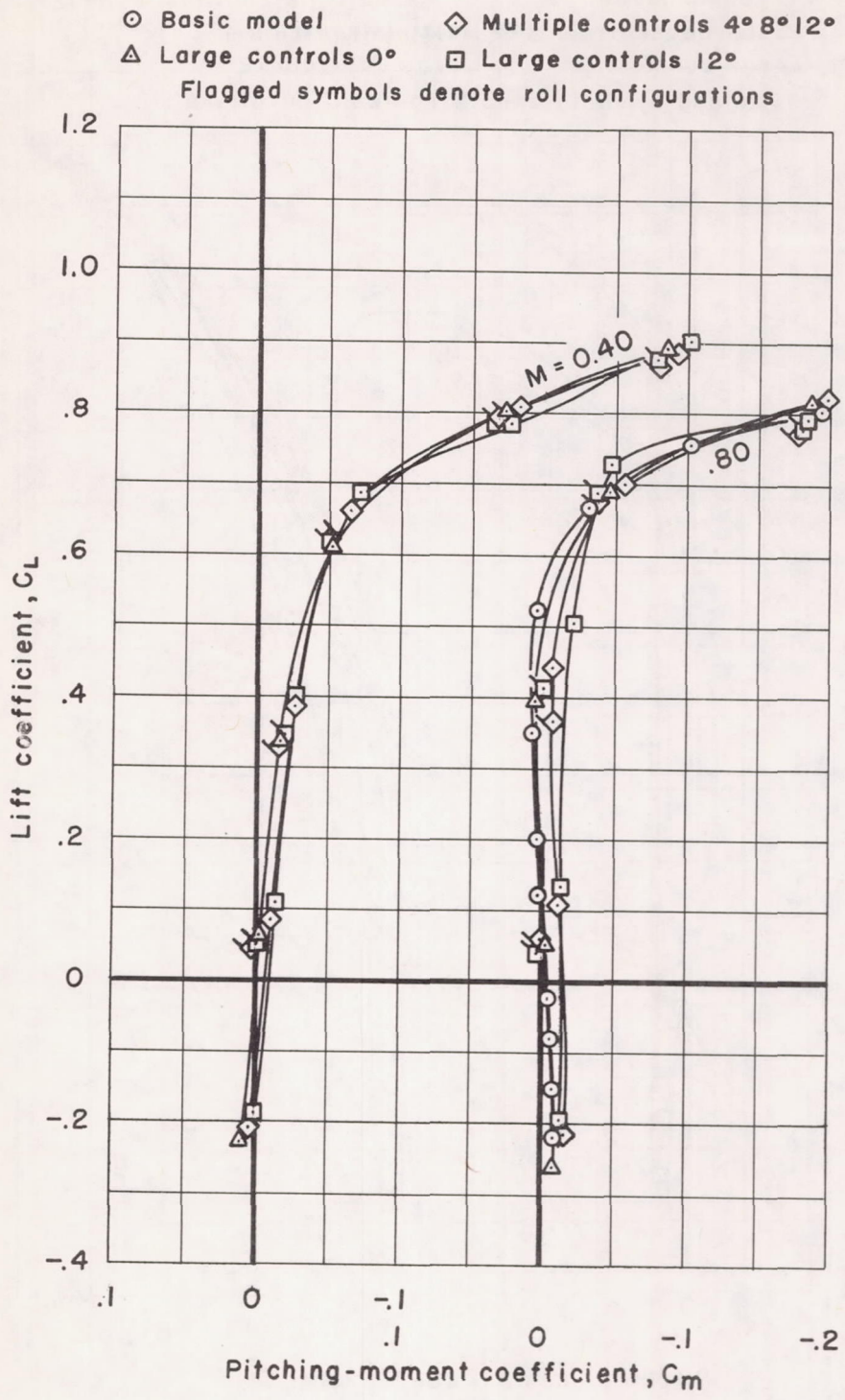

(a) M = 0.40; 0.80

Figure 14.- Variation of pitching-moment coefficient with lift coefficient for the model with and without combined upper and lower controls.

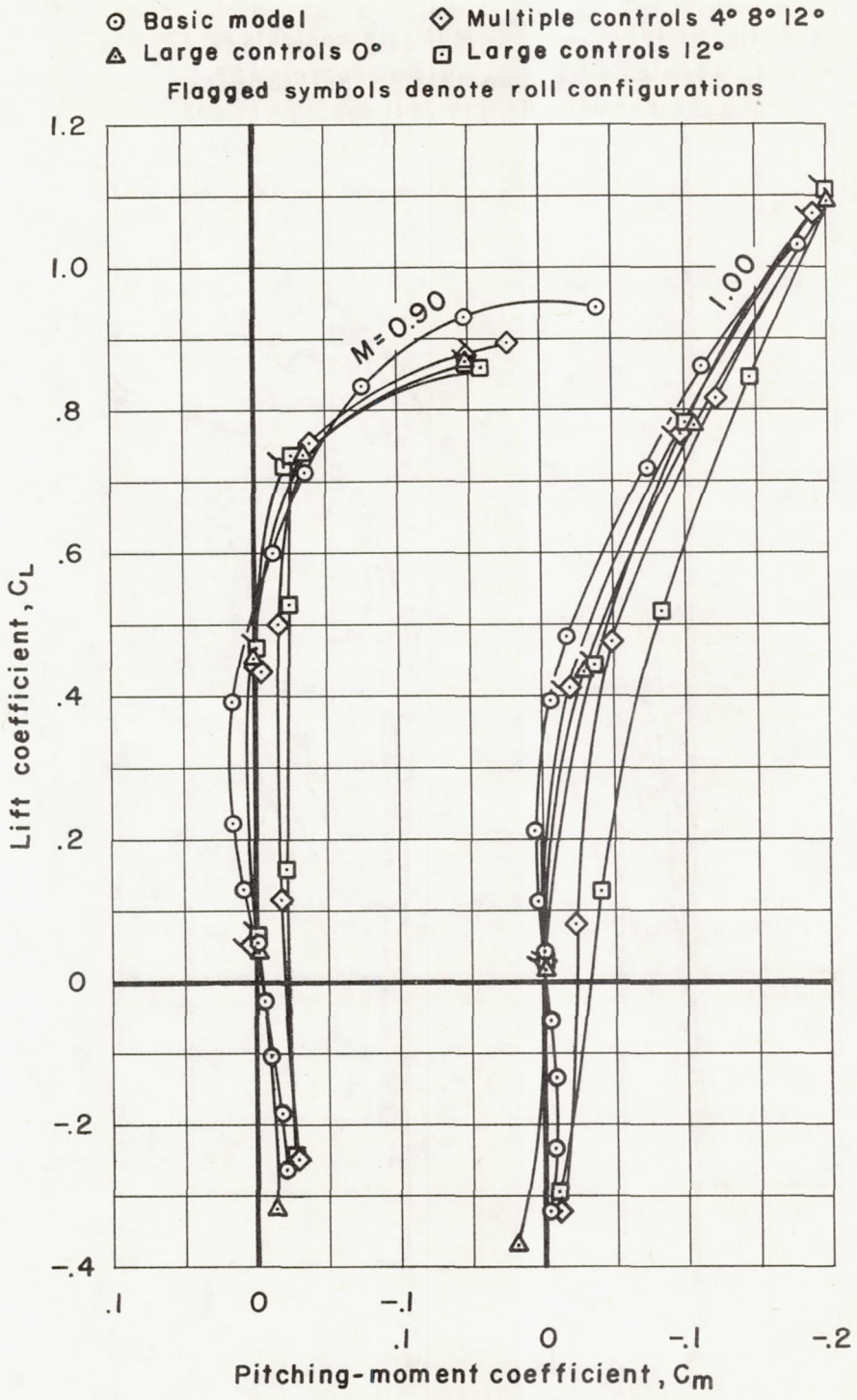

(b) M = 0.90; 1.00

Figure 14.- Continued.

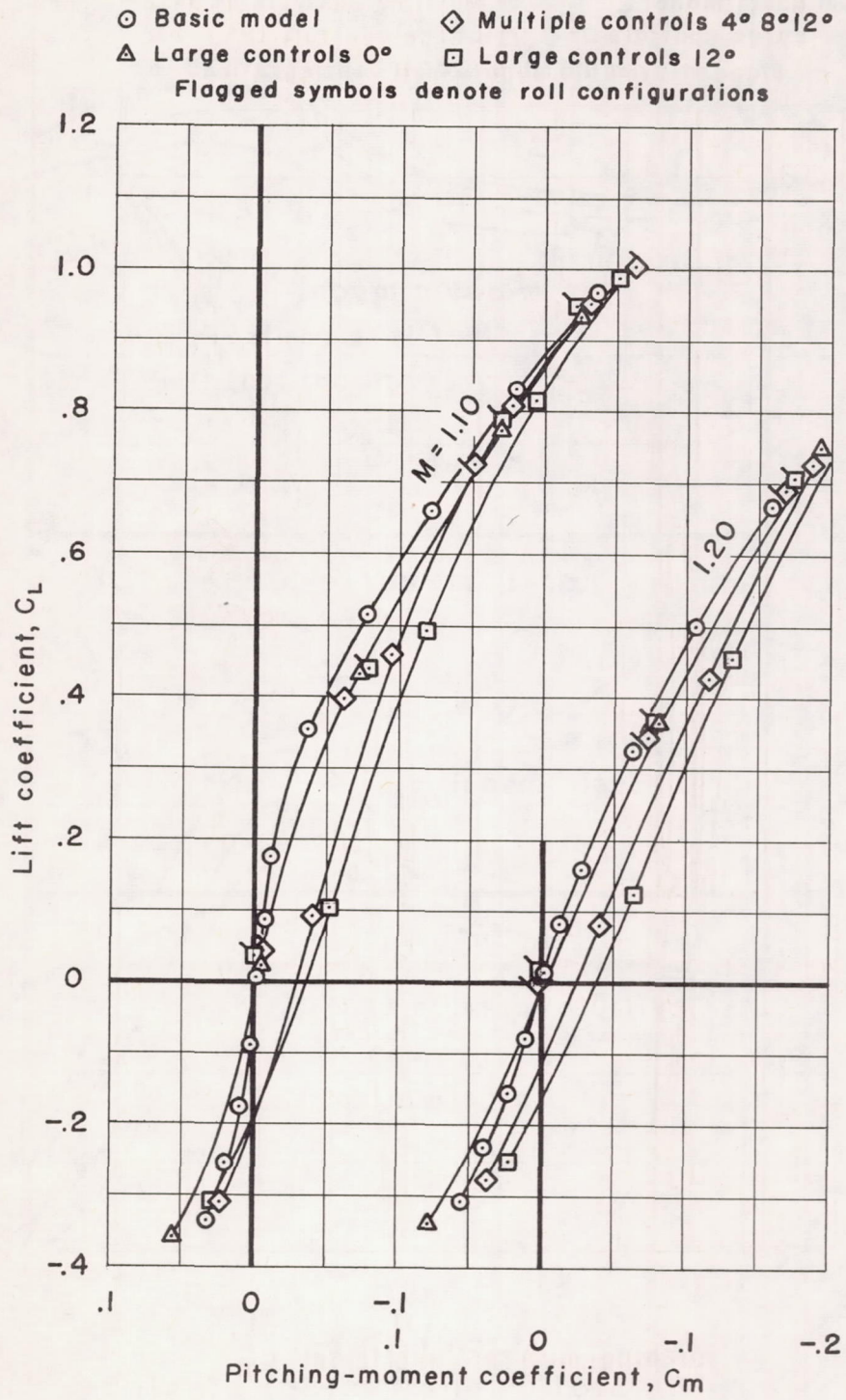

(c) M = 1.10; 1.20

Figure 14.- Concluded.

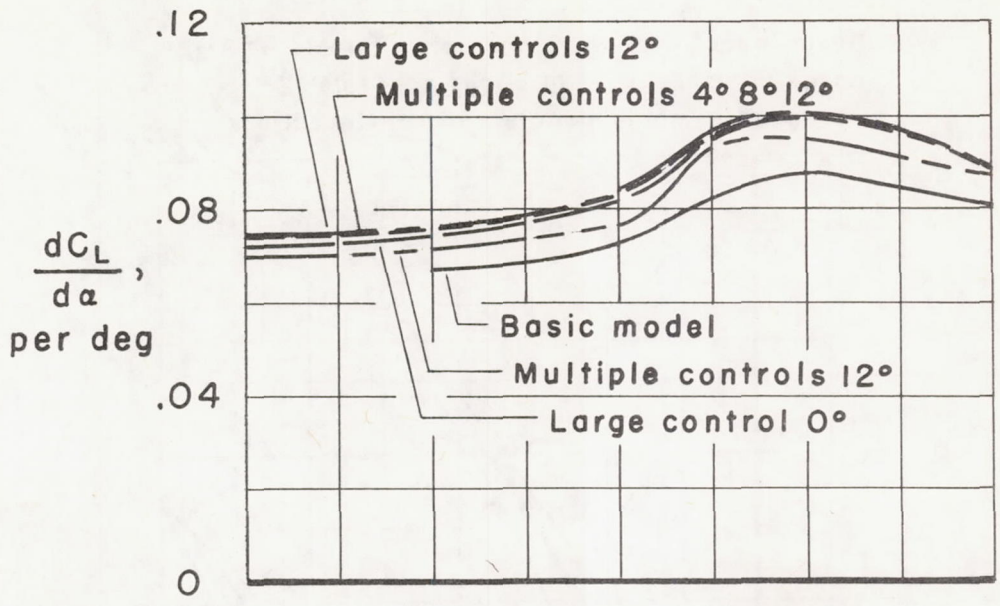

(a) Lift-curve slope.

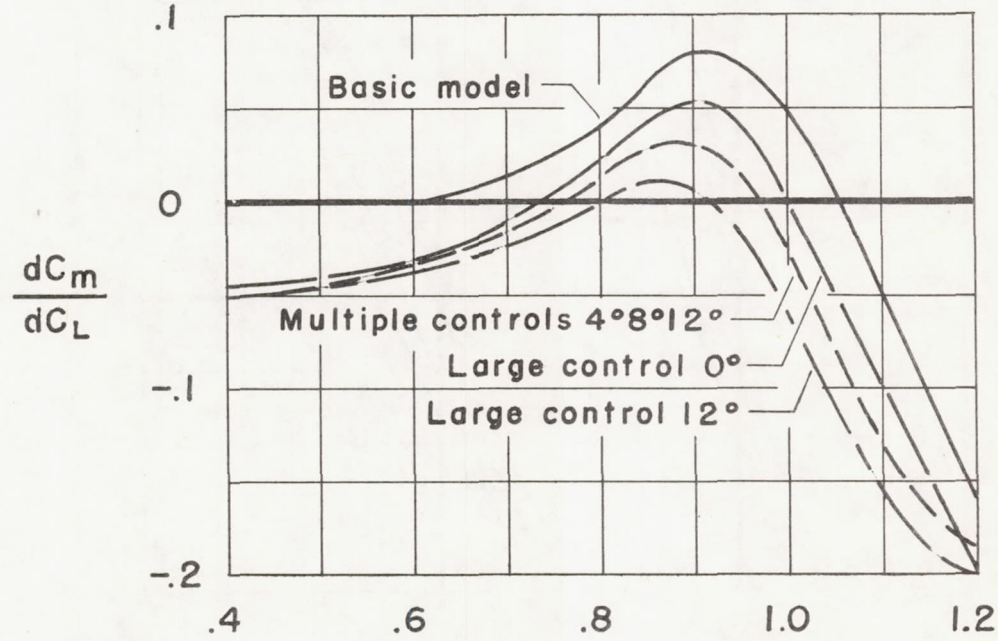

(b) Static longitudinal stabliity.

Figure 15.- Variations of lift-curve slope and static longitudinal stability for the model with and without combined upper and lower controls.

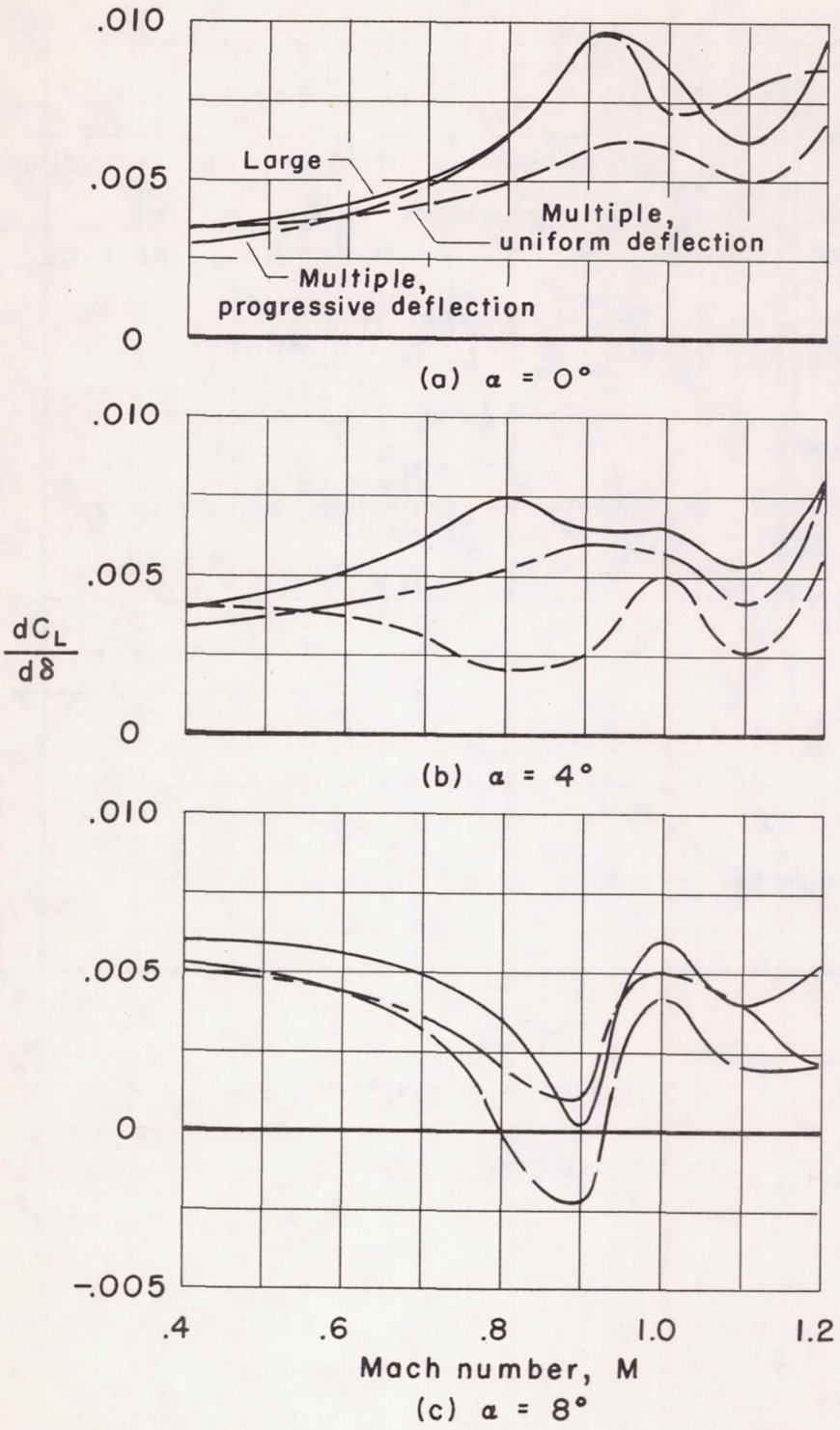

Figure 16.- Variation of lift-effectiveness parameter with Mach number for the combined upper and lower large controls and multiple controls.

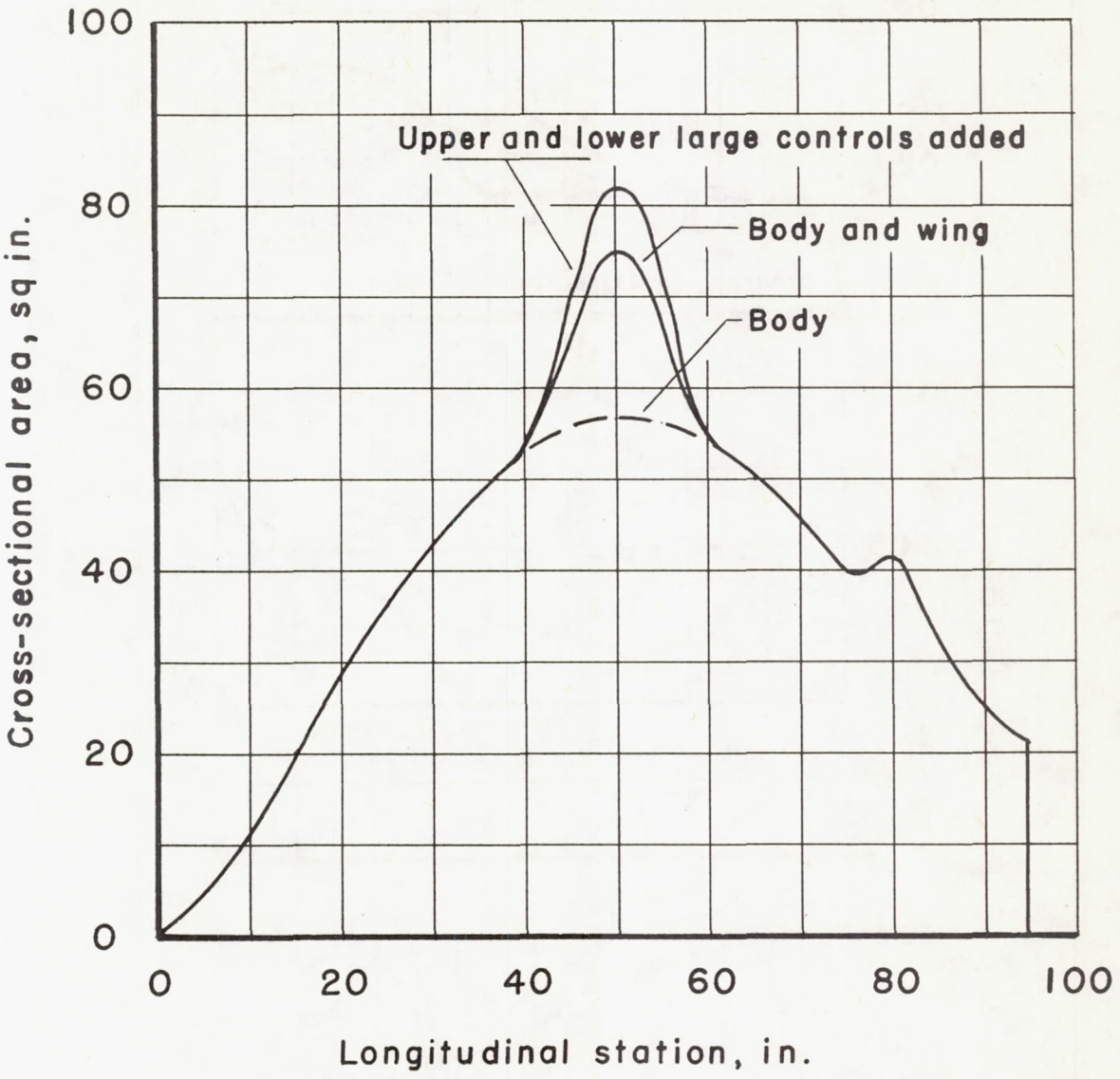

Figure 17.- Longitudinal distribution of cross-sectional area.

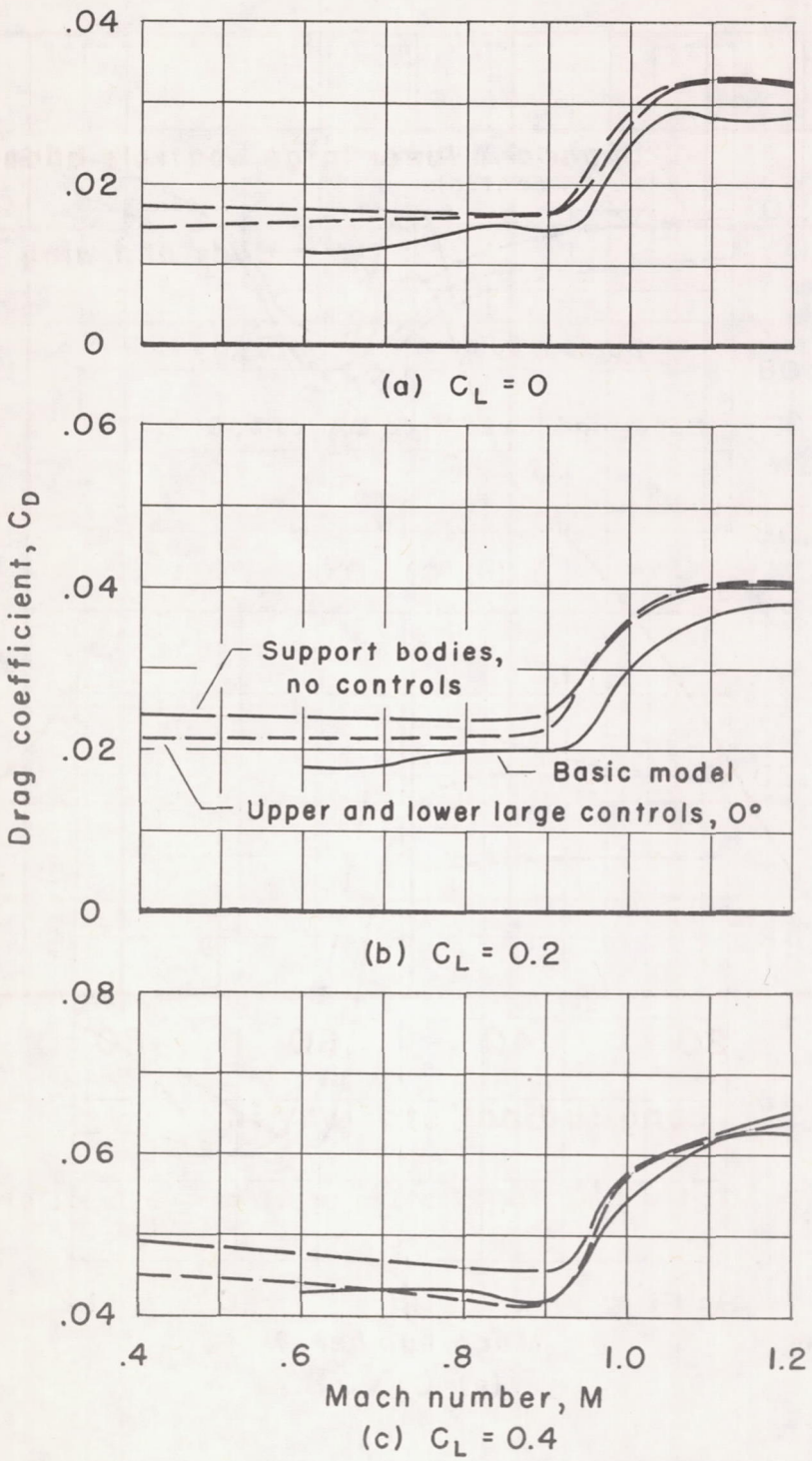

Figure 18.- Variation of drag coefficient with Mach number for the model with and without combined upper and lower large controls and support bodies.

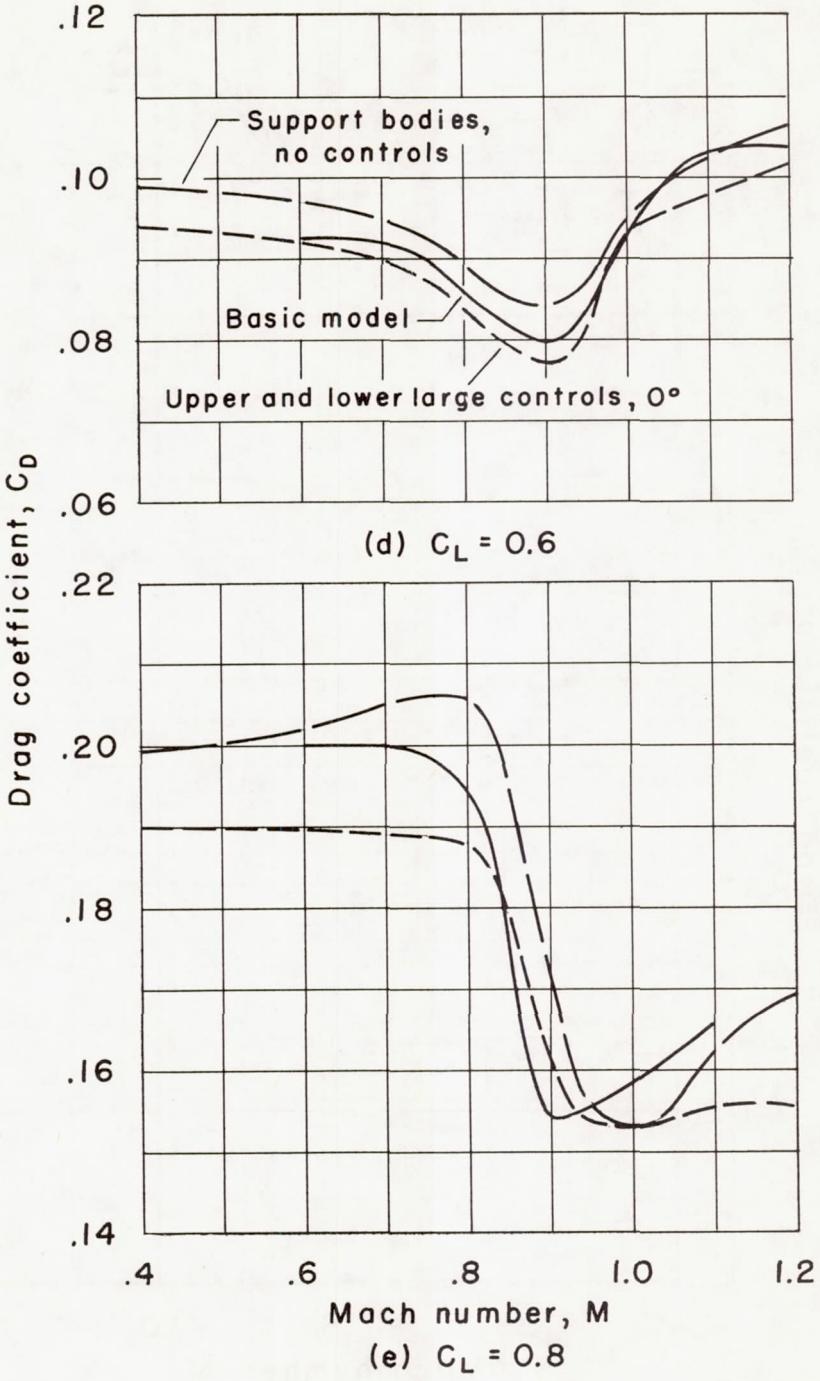

Figure 18.- Concluded.

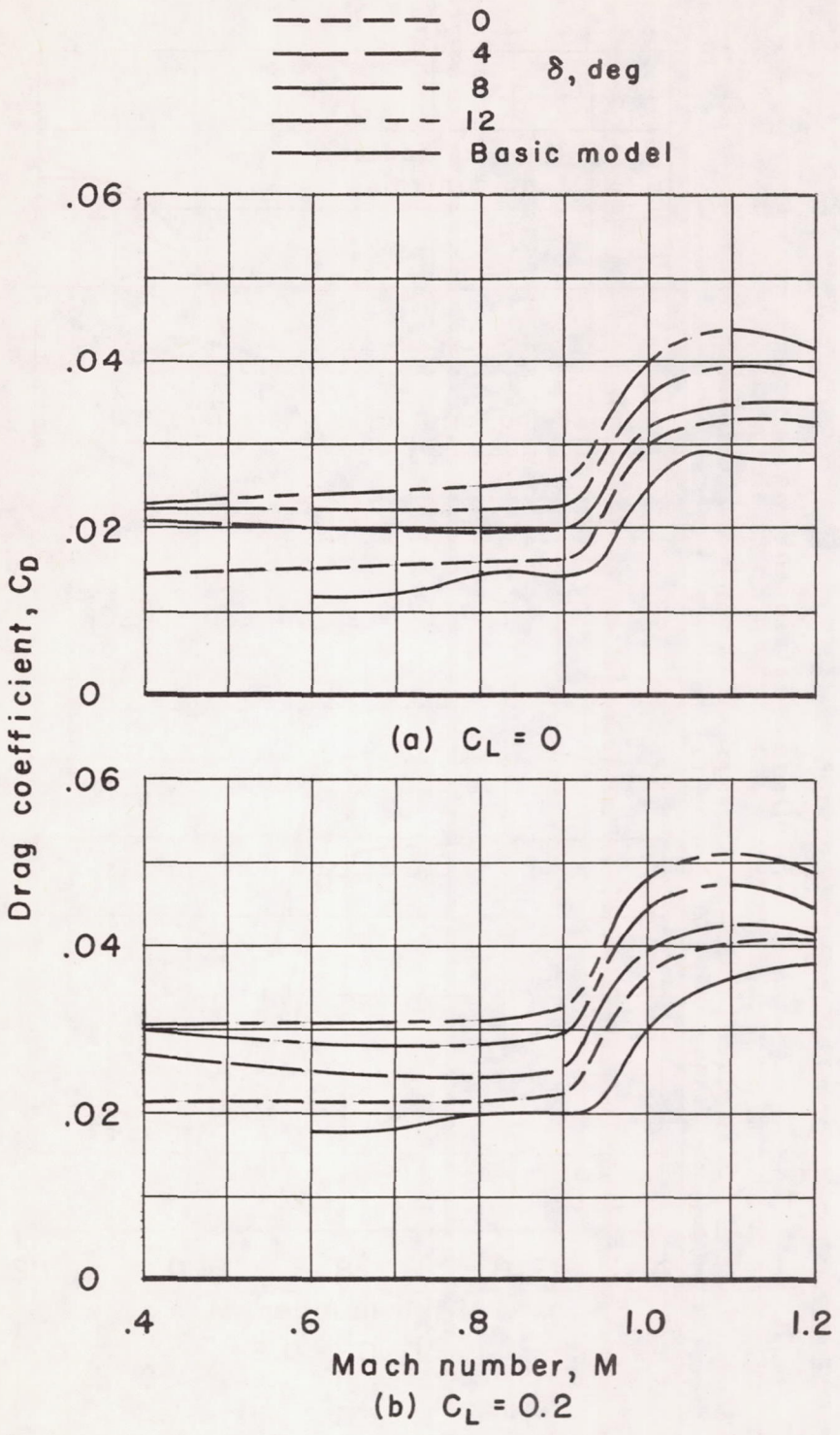

Figure 19.- Variation of drag coefficient with Mach number for the model with combined upper and lower large controls deflected to produce incremental lift.

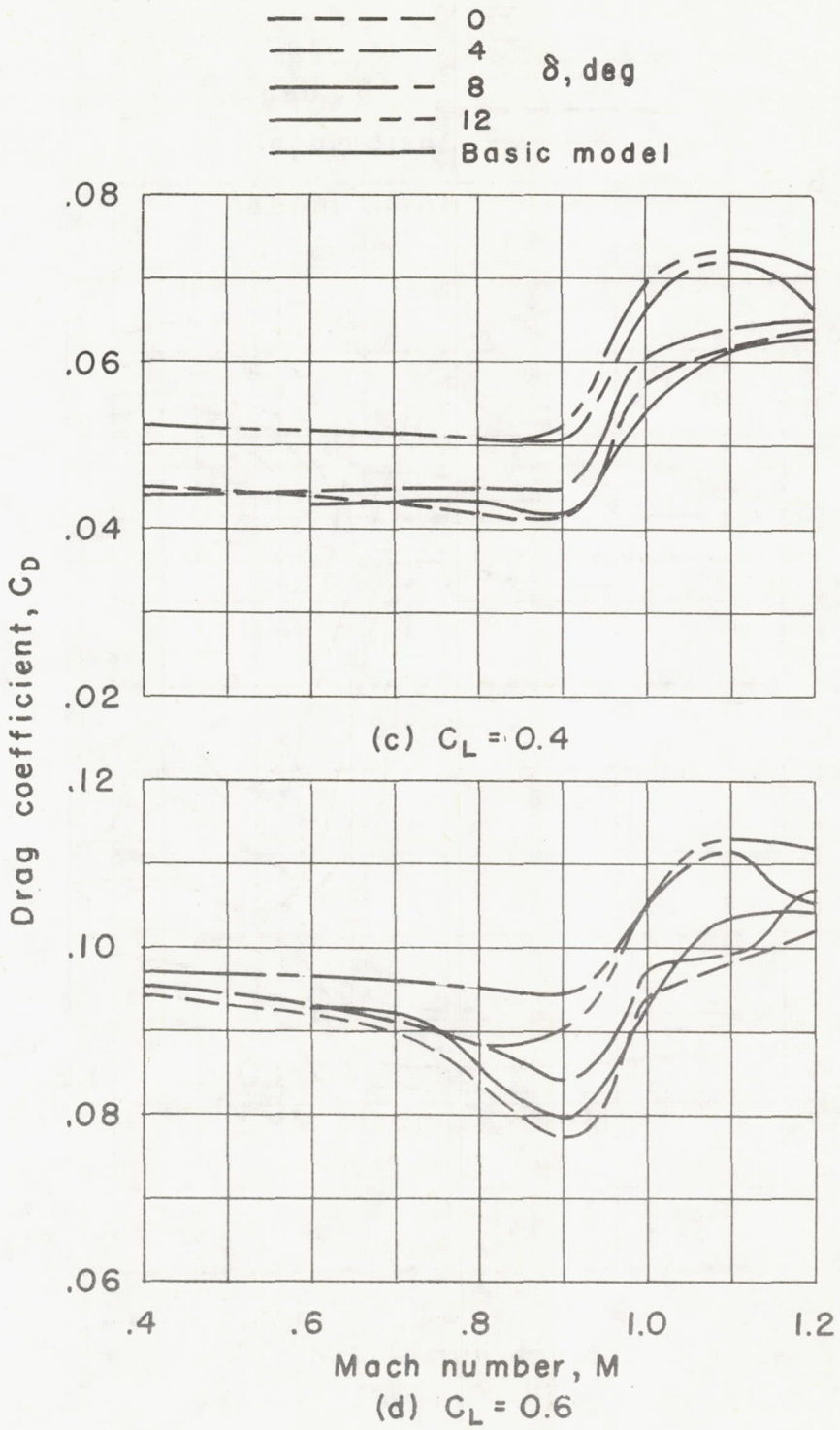

Figure 19.- Continued.

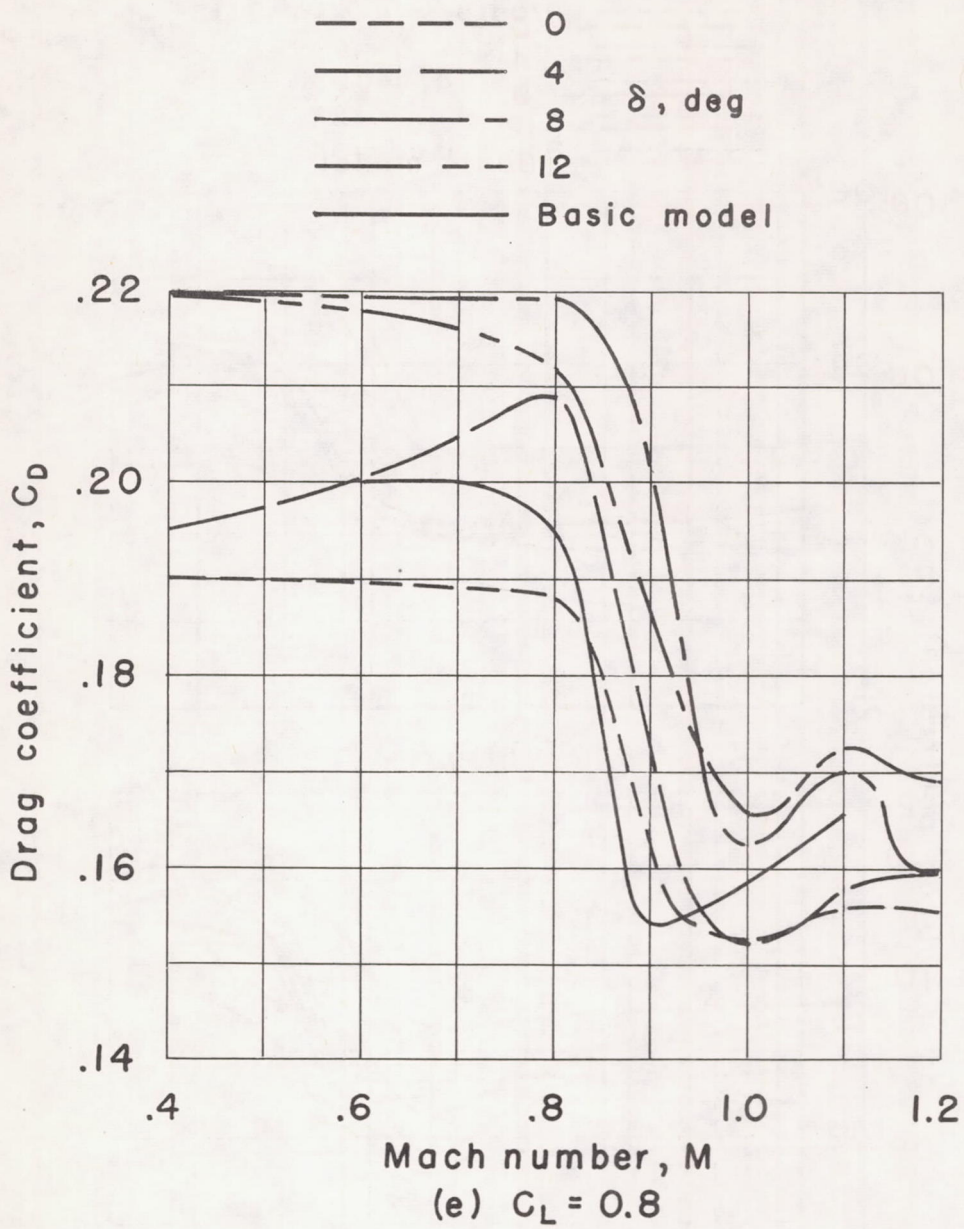

Figure 19.- Concluded.

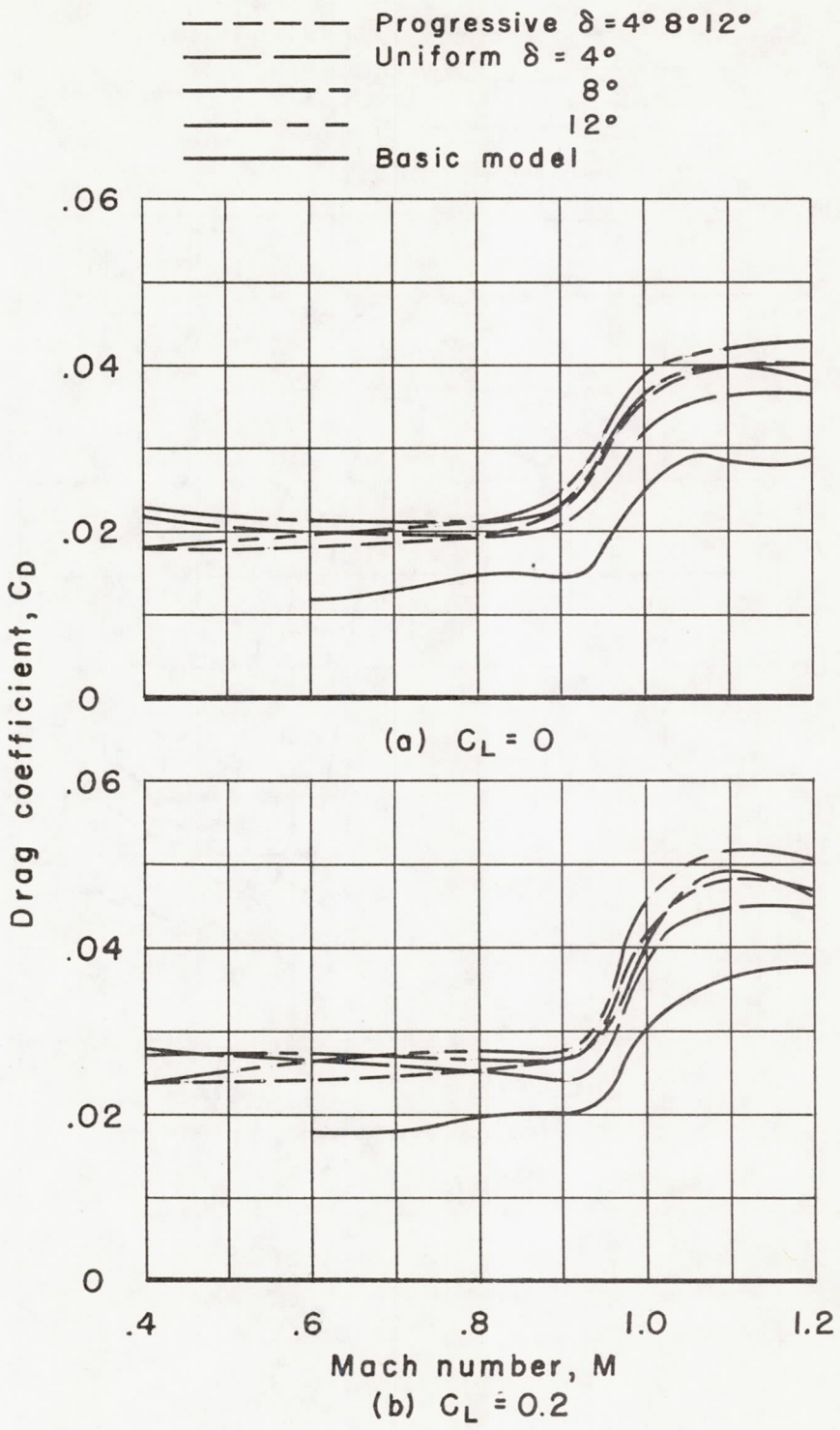

Figure 20.- Variation of drag coefficient with Mach number for the model with combined upper and lower multiple controls deflected to produce incremental lift.

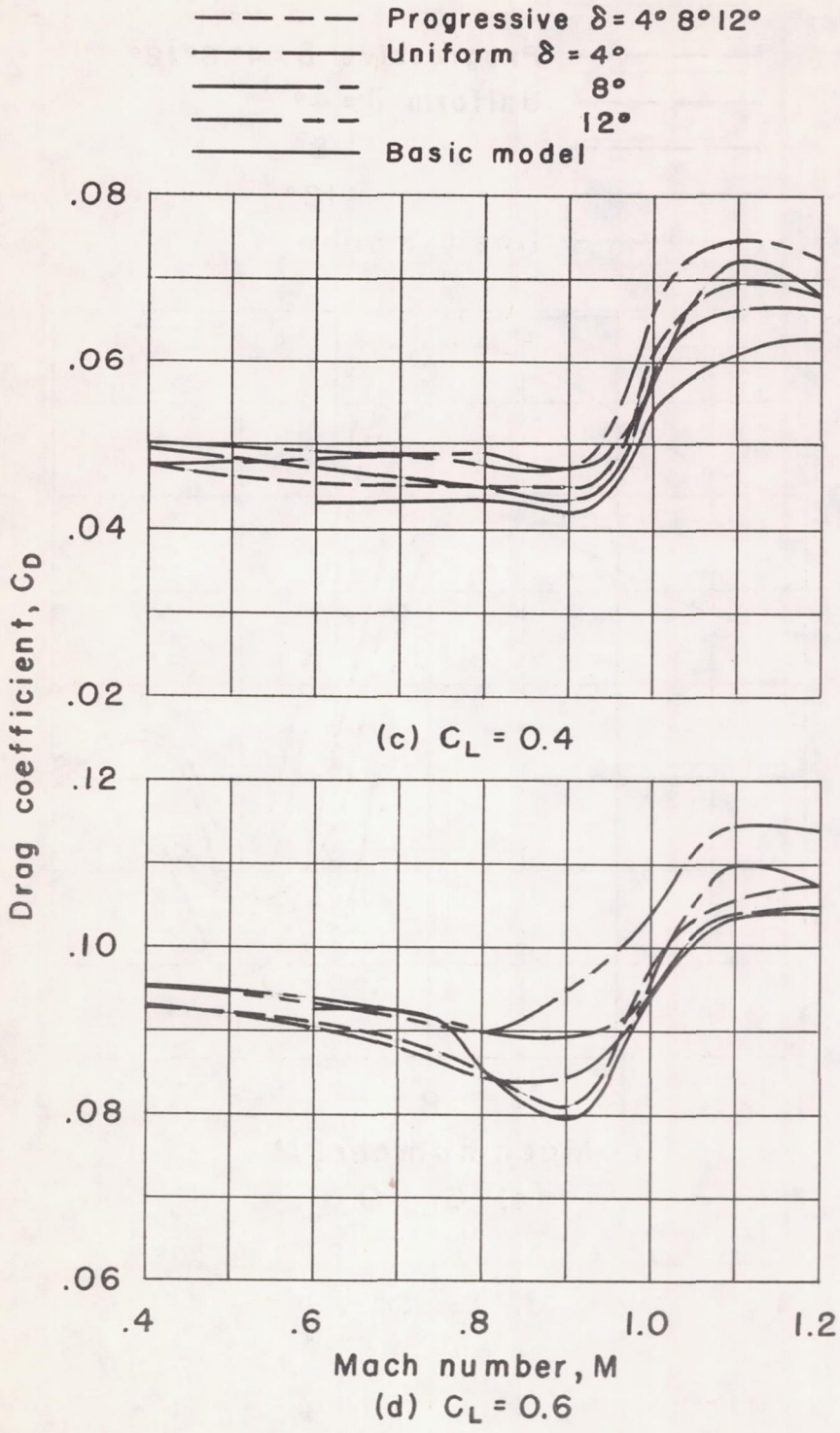

Figure 20.- Continued.

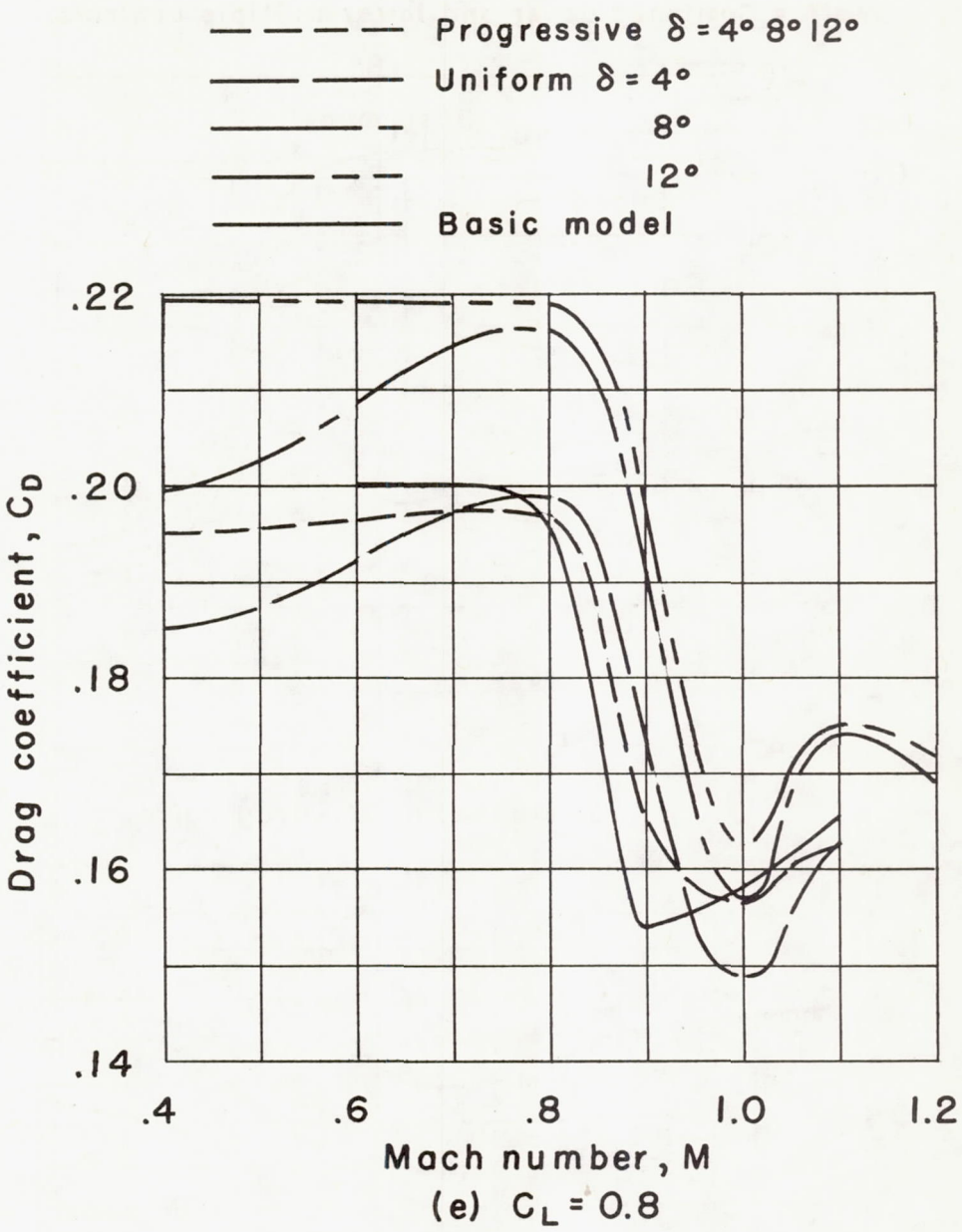

Figure 20.- Concluded.

Large = Combined upper and lower large controls.
Mult = Combined upper and lower multiple controls.

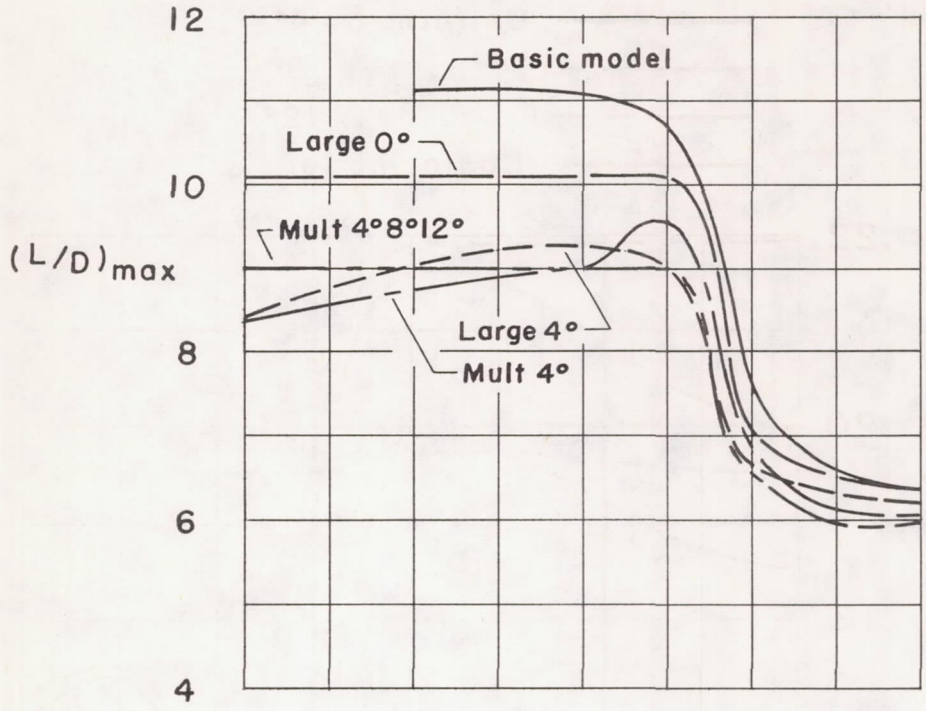

(a) Maximum lift-drag ratio.

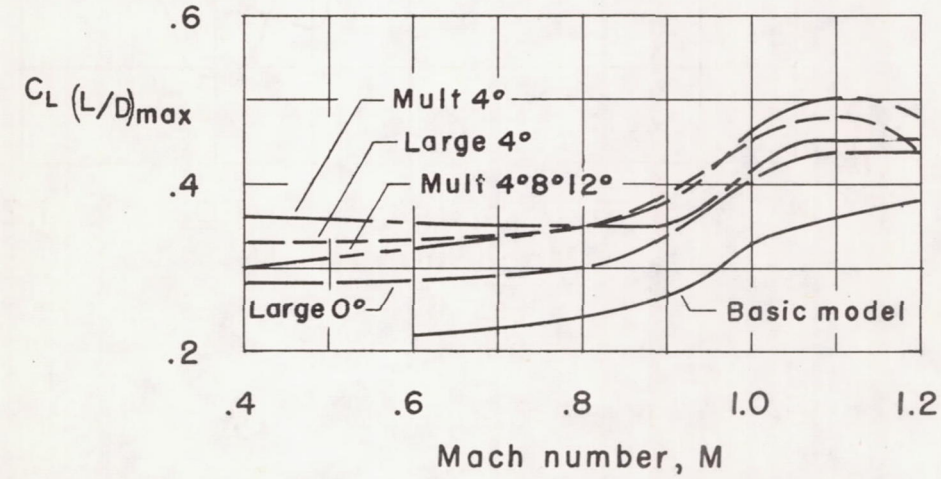

(b) Lift coefficient for maximum lift-drag ratio.

Figure 21.- Variations with Mach number of the maximum lift-drag ratio and the corresponding lift coefficient for several different control configurations.

CONFIDENTIAL